Received: 5 November 2025 | Accepted: 3 June 2026

DOI: 10.1111/1365-2656.70309

Journal of Animal Ecology

RESEARCH ARTICLE

Optimising daily sampling of plant–bee interaction networks

Caio S. Ballarin[1,2,3] | Jorge Isla[3] | Blanca Arroyo-Correa[3] | Elena Quintero[3,4] | Leandro Hachuy-Filho[1,5] | Felipe W. Amorim[1,2,5] | Pedro Jordano[3,4]

[1]Laboratório de Ecologia da Polinização e Interações—LEPI, Departamento de Biodiversidade e Bioestatística, Instituto de Biociências, Universidade Estadual Paulista "Júlio de Mesquita Filho" (UNESP), Botucatu, São Paulo, Brazil

[2]Programa de Pós-graduação Em Biologia Vegetal, Instituto de Biociências, Universidade Estadual Paulista "Júlio de Mesquita Filho", Botucatu, São Paulo, Brazil

[3]Integrative Ecology Group, Estación Biológica de Doñana, EBD-CSIC, Sevilla, Spain

[4]Departamento de Biología Vegetal y Ecología, Universidad de Sevilla, Sevilla, Spain

[5]Programa de Pós-graduação Em Zoologia, Instituto de Biociências, Universidade Estadual Paulista "Júlio de Mesquita Filho", Botucatu, São Paulo, Brazil

Correspondence
Caio S. Ballarin
Email: csballarin@gmail.com

Funding information
Coordenação de Aperfeiçoamento de Pessoal de Nível Superior, Grant/Award Number: 88887.839479/2023-00 and Finance Code 001; Fundação de Amparo à Pesquisa do Estado de São Paulo, Grant/Award Number: 2021/10639-5 and 2024/02640-1

Handling Editor: Paul CaraDonna

Abstract

1. Plant–pollinator interactions are dynamic not only across seasons but also over hourly time scales, even beyond the day–night contrast. However, capturing the daily temporal variability of pollination networks during field data collection is challenging. Consequently, our understanding of daily variation in network composition and structure remains incomplete due to limited sampling coverage. Moreover, inaccurate sampling protocols can result in missing links that impair the identification of underlying processes and emerging patterns. We address this gap by studying the fine-scale temporal organisation of the diverse diurnal plant–bee relationships and examining how the interaction composition and network structure fluctuate throughout the day.
2. We extensively sampled plant–bee interactions in a Brazilian Cerrado over two flowering seasons, encompassing six 2-h sampling periods throughout the day. We compared interaction β-diversity and network structural properties across sampling periods. A factorial approach was used to merge interactions among all combinations of sampling periods to assess how the composition and structure of the partial-day networks deviated from those exhibited by the full-day network (i.e. consolidating all interactions).
3. Plant–bee interactions exhibited notable variations in network metrics across daily sampling periods. From dawn to dusk, plant–bee networks showed reduced modularity and specialisation but greater nestedness. Interaction β-diversity between sampling periods increased progressively with wider temporal intervals, mainly explained by interaction rewiring among shared species. Combining four 2-h sampling periods recovered up to ~80% of all pairwise interactions and ~82% of interaction frequencies, and generated partial-day networks that most closely resembled the structure of full-day networks. These best-performing combinations consistently drew from daily central hours, whereas early-morning and late-afternoon periods contributed fewer but unique interactions.
4. Our study demonstrates that plant–bee interaction networks are time-sensitive at the intraday scale and that interaction completeness is not necessarily improved

Felipe W. Amorim and Pedro Jordano—co-senior author.

by increasing effort within a single time window, but rather by distributing sampling across, or focusing on, the most informative periods of the day. We provide a general framework to evaluate how temporal sampling design affects network representativeness in systems where interactions depend on time-of-day.

KEYWORDS
diurnal network structure, dynamical network topology, neotropical savanna, resource utilisation patterns, sampling schedules

1 | INTRODUCTION

Virtually all ecological interactions are undersampled (Jordano, 2016; Vázquez et al., 2009), reflecting the inherent limitations of biodiversity sampling (Gotelli & Colwell, 2011; Magurran, 1988) and motivating the need to identify the sources of such undersampling and its potential biases. One reason for incomplete interaction inventories is that interactions are structured in space and time, reflecting circadian, phenological, and ontogenetic cycles, as well as spatial constraints on dispersal that confine interactions to specific spatiotemporal contexts. For instance, a pairwise interaction may occur only in specific habitats (e.g. canopy vs. understorey, or forest interior vs. edge) or time periods (e.g. summer vs. winter or morning vs. afternoon) and be absent otherwise (Jordano, 2016; Olesen et al., 2011).

When ecological networks are treated as static snapshots—by collapsing variation across space and time—interaction patterns and emergent structural properties are assumed fixed, limiting our ability to identify processes shaping interactions, and to predict system responses to environmental change (Poisot et al. 2015; Fründ et al., 2016; Vizentin-Bugoni et al., 2016). Selecting representative spatiotemporal slices that capture the dynamic behaviour of species interactions is, thus, crucial for studying underlying processes and observed patterns in ecological interaction assemblages, as they may manifest significant variation across spatiotemporal scales and contexts (CaraDonna et al., 2021; CaraDonna & Waser, 2020; Levin, 1992; Olesen et al., 2008, 2010; Schwarz et al., 2020).

A major source of bias underlying discrepancies between realised and potential interactions is the temporal uncoupling among interacting organisms (Jordano, 2016). Contemporary ecology increasingly recognises that ecological interactions vary across temporal scales, and choosing an appropriate temporal resolution is essential to reveal scale-dependent patterns (Basilio et al., 2006; CaraDonna & Waser, 2020; Schwarz et al., 2020). For example, ecological networks reveal different dynamics across temporal scales, from interannual turnover driven by species migration and extinction at yearly scales (Alarcón et al., 2008; Resasco et al., 2021), to seasonal shifts driven by phenology within years (Arroyo-Correa et al., 2020; Basilio et al., 2006; Bramon Mora et al., 2020; CaraDonna et al., 2017), resource-use flexibility and rewiring across months (CaraDonna & Waser, 2020; Olesen et al., 2008) and circadian interaction patterns within days (Baldock et al., 2011; Nagano, 2023; Ratoni et al., 2025). Although less studied, daily variation in interaction patterns is important for understanding within-day ecological dynamics, offering fine-scale insights into interaction patterns (Herrera, 2024), particularly in systems involving ectothermic insects, where activity and foraging respond to temperature and rapid changes in resource availability.

Plant–pollinator interaction networks exhibit highly dynamic topologies at daily temporal scales (i.e. Baldock et al., 2011; Nagano, 2023; Ratoni et al., 2025). Intraday changes in interaction networks are expected to emerge from the joint effects of (i) daily rhythms in floral display and reward production (Ballarin et al., 2022), (ii) interspecific differences in pollinator circadian activity and microclimatic sensitivity (Herrera, 2024; Polatto et al., 2014; Stone et al., 1988) and (iii) shifts in the competitive environment as the identity and density of foragers and available resources change throughout the day (Ballarin et al., 2022). These processes imply that different periods of the day represent distinct ecological states of the same community, rather than incomplete samples of a single static network. Consequently, assuming temporal invariance overlooks shifts in interaction strength and resource partitioning, masking how network structure emerges through interaction rewiring and turnover. Static descriptions may therefore misrepresent network structure, attributing differences between networks to environmental drivers when they instead reflect differences in temporal sampling. For example, a pollination network may appear highly specialised if sampling captures periods of strong niche partitioning and floral constancy, even though interactions shift and competition relaxes throughout the day. Even a single missed interaction may distort estimates of, for example, specialisation and disturbance propagation within mutualistic networks.

However, surveys of plant–pollinator interactions usually sample only a subset of daily hours or ignore the timing of each interaction (see Baldock et al., 2011). Although the importance of daily timing is widely acknowledged (Baldock et al., 2011; Nagano, 2023; Ratoni et al., 2025), we still lack a clear understanding of how pollination network structure and interaction composition change across the day and how this affects sampling reliability. Plant–bee interactions are particularly suitable for this purpose because intraday shifts in bee activity and flexible resource use promote frequent interaction turnover and rewiring. Here, using a high-resolution plant–bee interaction network sampled at six 2-h intervals (1440 h in total), we (i) quantified how network structure and the identity of pairwise interactions differ among daily sampling periods. To propose field strategies that minimise daily sampling efforts while ensuring interaction data completeness, we

then (ii) evaluated all possible combinations of 2-h intervals to identify sampling schedules that maximise interaction completeness and best recover the full-day network, used as a benchmark. Finally, we assessed which network metrics are least sensitive to incomplete daily sampling and therefore better preserve information about network structure under reduced sampling effort.

Based on this framework, we hypothesised that both network structure and interaction composition should change predictably across the day, primarily through extensive interaction rewiring rather than species turnover. This expectation follows from the fact that most plants and bees co-occur throughout the day but adjust their foraging and visitation patterns in response to intraday changes in floral resource presentation and microclimatic conditions, leading the same species to interact with different partners at different times (Arroyo-Correa, 2025; Ratoni et al., 2025). We further hypothesised that sampling schedules including the central daylight hours, when temperature and bee activity are highest, floral overlap is maximal, and resources are not yet strongly depleted, should maximise interaction completeness and best approximate full-day network structure. Finally, we expected that network metrics based on interaction frequencies would be less sensitive to incomplete daily sampling, as observed for increasing temporal sampling effort in other contexts (e.g. Vizentin-Bugoni et al., 2016).

2 | MATERIALS AND METHODS

2.1 | Study site and data collection

This study was carried out in a Cerrado area situated in the Botucatu municipality, São Paulo state, Brazil (34 ha; 22°56′20″ S, 48°27′29″ W; 860 m a.s.l.), characterised by the predominance of herbaceous/grassy vegetation interspersed with scattered trees and shrubs. The plant community comprises functionally diverse species with contrasting phenologies, daily flower-opening schedules, resource types, shapes and colours, with most species being visited by bees even when these are not their primary pollinators (see Ballarin et al. 2025; Ballarin, Amorim, et al. 2026; Ballarin, Fidelis, et al., 2026). To sample empirical plant–bee interactions, we conducted weekly visual censuses over two consecutive flowering seasons (2021/2022–2022/2023) across 12 100 m^2 (10 × 10 m) plots spaced at least 30 m apart, during the peak of angiosperm flowering (mid-July to early March). Each census consisted of recording interaction events in six 2-h intervals, divided over two consecutive days, based on local clock time: from 06:00 to 12:00 on the first day and from 12:00 to 18:00 on the second day. Sampling days were selected to ensure similar weather conditions (e.g. temperature, cloud cover and wind), and the 2-h intervals were adopted to allow all plots to be surveyed within each period and to minimise the influence of seasonal variation in sunrise and sunset on the earliest and latest intervals. During each observation period, we sampled all bee-pollinated flowering plant species within each plot (ca. 90% of all animal-pollinated species; Ballarin, Fidelis, et al., 2026) using a plant-focused protocol. Groups of nearby flowering individuals were observed for 5 min, and we recorded the number of legitimate bee visits (i.e. visits contacting reproductive structures; $n = 720$ h per flowering season). Our sampling encompassed all bee taxa visiting flowers in plots, including taxa foraging on distinct resources, and species with both temporally restricted (e.g. *Ptiloglossa*) and broad (e.g. *Apis mellifera*) daily activity patterns, reflecting a dataset sensitive to sampling time (Table S1). Bee specimens not reliably identified in the field were collected for later taxonomic identification after floral visits. Collection and identification of bee specimens were conducted under SISBIO/ICMBio authorisation number 75978-1, and fieldwork was authorised by the municipal authority responsible for the study area. No animal ethics committee approval was required for the invertebrate sampling involved in this study. To mitigate potential biases associated with sampling periods, we varied the order of plot surveys among sampling days.

2.2 | Composition and structure of empirical networks across sampling periods within the day

We created matrices M_t, where elements m_{ijt} represent the frequency of legitimate interactions between a particular plant species i and a specific bee species j at daily time interval t. To assess variation in network structure according to the daily period of data sampling, we constructed 144 interaction networks, with each network including the aggregated interaction frequencies between plants and bees in a given 2-h sampling period/plot/flowering season ($n = 24$ plant–bee networks—M_t—for each 2-h sampling period). Thus, each 2-h period was sampled in 12 plots per season across two seasons, totalling 240 h per period. Interaction richness estimates for each sampling period indicated a coverage of 72.33 ± 3.27% (mean ± SD; Figure S1) of all potential pairwise plant–bee interactions (Chao 1 estimator, 'iNEXT' package—version 3.01; in R—version 4.4.2; Chao, 1984; Chacoff et al., 2012; Hsieh et al., 2016). Sampling completeness varied among networks built for each period and plot, with the 16:00–18:00 period consistently showing lower completeness ($\chi^2_{139,5} = 22.76$; $R^2\text{-}_{adjusted} = 0.70$; $p < 0.01$; Figure S1).

We then evaluated whether patterns of plant–bee interactions differ across 2-h sampling periods using different network descriptors. Pairwise interaction richness was calculated as the number of unique pairwise plant–bee interactions. Connectance (*C*) computes the proportion of realised out of all potential interactions. Interaction evenness (*IE*) assesses the uniformity of interaction distribution. Specialisation degree (*H2′*) measures the degree of specialisation by considering partner availability and interaction exclusiveness (Blüthgen et al., 2006). Weighted nestedness (*wNODF*) evaluates whether interactions of any given species form a proper subset, nested within those of the more generalist ones; higher *wNODF* values indicating greater nestedness. Weighted modularity (*Qw′*) was computed using the DIRTLPAwb+ algorithm (Beckett, 2016) and indicates whether the network is structured into modules with denser within- than between-module interactions (Olesen et al., 2007). *C*, *IE*, *H2′* and *Qw′* range from 0 to 1, with values closer to 1 indicating high network connectance, interaction evenness, specialisation and

modularity, respectively. For *wNODF* and *Qw′* metrics, we applied a Δ-transformation by subtracting the mean value of random networks generated by a null model from empirical values. Δ*wNODF* and Δ*Qw′* were used to correct deviations unrelated to network structure, enabling the comparison among networks with different sizes and connectance (Fründ et al., 2016). We used the Patefield algorithm to generate the null matrices, which preserves species richness and the total number of interactions (Patefield, 1981). All network metrics were assessed using the 'bipartite' package in R (Dormann et al., 2008; version 2.20).

Finally, we computed dissimilarities (i.e. β-diversity) among plant–bee interaction networks across sampling periods. To preserve compositional differences among plots and flowering seasons, β-diversity was assessed only among periods within the same plot and season, yielding 15 pairwise comparisons per plot and season ($n=360$ comparisons across all periods, plots and seasons). To calculate interaction β-diversity, we used the quantitative Ruzicka distance coefficient, which incorporates interaction frequencies among shared links between compared networks (Magrach et al., 2017). Three components of β-diversity were calculated: β^{OS}, reflecting changes in interaction composition among shared species (i.e. rewiring); β^{ST}, representing interaction dissimilarities due to species turnover between sampling periods (i.e. turnover; Poisot et al., 2012); and β^{WN}, quantifying the overall interaction dissimilarity between compared networks. β^{ST} and β^{OS} are additive components of total interaction β-diversity, such that $\beta^{WN}=\beta^{ST}+\beta^{OS}$. Values range from 0 to 1, with 1 indicating higher temporal β-diversity in plant–bee interactions.

We fitted mixed models to test whether network structure and interaction composition differ among sampling periods. Network structure was analysed using separate models for each metric (pairwise interaction richness, *C*, *IE*, *H2′*, *wNODF* and *Qw′*), with the 2-h sampling period as a categorical predictor. Interaction composition was evaluated by modelling β-diversity, with β^{WN} as the response and the comparison between sampling periods as a categorical predictor, and by quantifying the contributions of β^{OS} and β^{ST}. In all models, plot identity and season were included as crossed random effects to account for non-independence arising from repeated observations across all plot–season combinations, and pairwise contrasts were assessed with Tukey tests using 'emmeans' R package (Lenth, 2016; version 1.10.3). Model details are given in Table S2.

2.3 | Merging interactions into partial- and full-day networks

Besides comparing compositional and structural properties of plant–bee networks among 2-h sampling periods, we assessed how well single or combined periods represent the full daily network. Given our extensive sampling ($n=1440$ h; 60 weeks), we used the pooled network across all sampling periods and plots (i.e. the full-day network) as the benchmark of representativeness. This benchmark encompasses the daylight period when bees forage on flowers and integrates interactions recorded over 30 weeks spanning most of the flowering season. Quantitative evaluation of sampling completeness indicated that this full-day network captured approximately 78% of the estimated total number of pairwise interactions (Figure S2). This approach ensured that the majority of plant–bee pairwise interactions were effectively sampled, thereby providing a robust basis for evaluating the representativeness of single (or combination of) sampling periods (i.e. partial-day networks) in representing the structure and composition of plant–bee interaction networks.

We adopted a factorial approach to combine sampling periods, considering all possible combinations. At this stage, networks were constructed by pooling all plots to minimise spatial bias due to differences in plant composition among plots. To assess fine-scale compositional and structural differences across sampling periods, we treated networks from each flowering season as independent sampling units, accounting for interannual variation in plant and bee composition. We generated 126 networks by merging all combinations of sampling periods within each flowering season ($n=62$ partial-day and one full-day network per flowering season).

2.4 | Assessing the structural and compositional representativeness of partial-day networks

We subsequently estimated pairwise interaction richness, *C*, *IE*, *H2′*, *wNODF* and *Qw′*, to assess how representative each partial-day network is relative to the full-day network. Despite high sampling coverage, rare interactions may still have been missed due to the absence of particular species, potentially biasing the identification of the most representative partial-day networks (see Dorado et al., 2011; Jordano, 2016). To account for this potential bias, we generated 1000 null matrices with the Patefield algorithm to compare the representativeness of each partial-day network in delivering information of the properties of the network (e.g. pairwise interaction richness, *C*, *IE*, *H2′*, *wNODF* and *Qw′*; see Vizentin-Bugoni et al., 2016 for a similar approach). We relaxed the network connectance in the generation of null matrices, which is fixed in other algorithms, such as 'vaznull' and 'swap.web', allowing for variability in the relative number of different pairwise interactions during our simulations. For pairwise interaction richness and *Qw′*, we worked only with 100 randomisations due to the extensive computation time required owing to the additional iterations those algorithms present. This procedure allowed us to compare combinations of sampling periods and select partial-day networks whose topology most closely matched the full-day network. To quantify similarity, we extracted z-scores for each network metric using null matrices ($n=124{,}000$ [or 12,400]: 1000 [or 100] for each of the 62 combinations per flowering season, excluding the full-day network). Z-scores measured deviations of each partial-day network from the full-day network mean. Partial-day networks with z-scores close to zero were therefore the most topologically similar to the full-day network. We also computed the mean β^{WN} of plant–bee interactions between each partial-day network and the full network within each flowering season. Because the full-day network includes the largest number of unique interactions, this allowed us to identify which single or combined sampling periods best

represent daily interaction assembly. Partial-day networks with the lowest mean β-diversity were therefore those capturing most existing plant–bee interactions.

2.5 | Identifying network metrics less sensitive to varying sampling effort

Finally, to determine how many 2-h sampling periods are needed to capture network properties across the full daylight span, we grouped partial-day and full-day networks (from one to six joint sampling periods) into six treatments representing sampling duration. We also treated network type (empirical vs. null) as a factor to assess how many periods are required to obtain metric values unlikely to arise by chance (Vizentin-Bugoni et al., 2016). We then visually inspected how network metrics (pairwise interaction richness, *C*, *IE*, *H2′*, *wNODF*, *Qw′*) changed in empirical and null matrices as sampling periods were added. This analytical procedure allowed us to evaluate: (i) whether the estimated network metrics effectively preserve information about plant–bee interaction networks following the addition of sampling periods; and (ii) what network metric needs less sampling resolution to deliver scores that deviate from null expectations.

2.6 | Intra- and inter-seasonal consistency of daily interaction patterns

Because flowering and pollinator phenology vary markedly across the season in the Cerrado (Ballarin, Amorim, et al. 2026; Ballarin, Fidelis, et al., 2026), we evaluated whether patterns across daily sampling periods remained consistent under different seasonal contexts. We assessed temporal consistency in interaction frequency and pairwise interaction richness across sampling weeks, phenological blocks (early-, mid- and late-season), and flowering seasons, and repeated all core analyses—including network metrics, interaction β-diversity and the representativeness of partial-day networks relative to full-day networks—across phenological blocks and flowering seasons. This allowed us to test whether seasonal turnover in species composition and interaction frequencies influenced comparisons among daily sampling periods. Full methodological details are provided in the Supplementary Methods.

3 | RESULTS

We recorded 24,546 legitimate plant–bee interactions, of which more than half were detected during the mid-morning period (i.e. 08:00–10:00 and 10:00–12:00), and this pattern was consistent across plots (Table 1). Sampling periods from 08:00–10:00 to 12:00–14:00 presented the highest richness of interacting plant and bee species (Table 1). Plant–bee interaction richness and the number of unique pairwise interactions restricted to a single sampling period reached their highest values around midday (i.e. from 08:00–10:00 to 12:00–14:00), with approximately 370 different plant–bee interactions, about 15–18% of which were unique to each single

TABLE 1 Summary metrics of interactions comprised in plant–bee networks encompassing each specific 2-h time interval.

Sampling periods	Plant species richness	Bee species richness	Frequency of plant–bee interactions	% of interactions	Pairwise interaction richness	Unique pairwise interactions	% of unique pairwise interactions
6–8 h	74 (14.25 ± 2.86)	35 (12.15 ± 3.18)	3011 (125.46 ± 72.53)	12.27	236	24 (10.17%)	8.28
8–10 h	90 (23.21 ± 4.93)	47 (16.46 ± 3.75)	6130 (255.42 ± 155.36)	24.97	377	65 (17.24%)	22.41
10–12 h	92 (23.71 ± 4.89)	45 (16.61 ± 3.62)	7762 (323.42 ± 292.61)	31.62	369	57 (15.45%)	19.66
12–14 h	88 (22.37 ± 5.59)	45 (15.21 ± 3.50)	3971 (165.46 ± 89.25)	16.18	381	69 (18.11%)	23.79
14–16 h	78 (18.75 ± 4.77)	42 (14.04 ± 2.37)	2268 (94.50 ± 31.59)	9.24	329	40 (12.16%)	13.79
16–18 h	71 (14.01 ± 3.67)	41 (10.71 ± 2.68)	1404 (58.50 ± 27.61)	5.72	251	35 (13.94%)	12.07

Note: Mean ± SD in parentheses depicts values obtained for each plot. % values in parentheses represent the proportional score of unique pairwise interactions considering all inventories of plant–bee pairwise interactions within each sampling period.

period (Table 1). However, interactions occurring at the beginning and end of the day (i.e. 06:00–08:00or 16:00–18:00) still represented 20.35% of all unique pairwise interactions (Table 1).

3.1 | Composition and structure of empirical networks across sampling periods within the day

All network metrics differed between sampling periods, although each metric showed distinct temporal patterns across the day, indicating that daily periods of data sampling influence the structure of plant–bee networks. Pairwise interaction richness was higher near midday (i.e. from 8:00 to 14:00; $\chi^2_{5,139}=434.24$; $R^2_{adjusted}=0.80$; $p<0.01$; Figure 1a). Network connectance (*C*) was higher in the period nearing dusk (i.e. 16:00–18:00; $\chi^2_{5,139}=36.82$; $R^2_{adjusted}=0.26$; $p<0.01$; Figure 1b). Interaction evenness (*IE*) and weighted nestedness (*ΔwNODF*) increased consistently throughout the day, being significantly higher during sampling periods after midday (*IE*—$\chi^2_{5,139}=76.62$; $R^2_{adjusted}=0.85$; $p<0.01$; Figure 1c; *ΔwNODF*—$\chi^2_{5,139}=103.82$; $R^2_{adjusted}=0.60$; $p<0.01$; Figure 1e). Network-wide specialisation degree (*H2′*) was higher in the early morning (i.e. 06:00–08:00; $\chi^2_{5,139}=74.73$; $R^2_{adjusted}=0.86$; $p<0.01$; Figure 1d). In contrast, the modularity (*Qw′*) of plant–bee networks decreased consistently throughout the day ($\chi^2_{5,139}=50.49$; $R^2_{adjusted}=0.60$; $p<0.01$; Figure 1f).

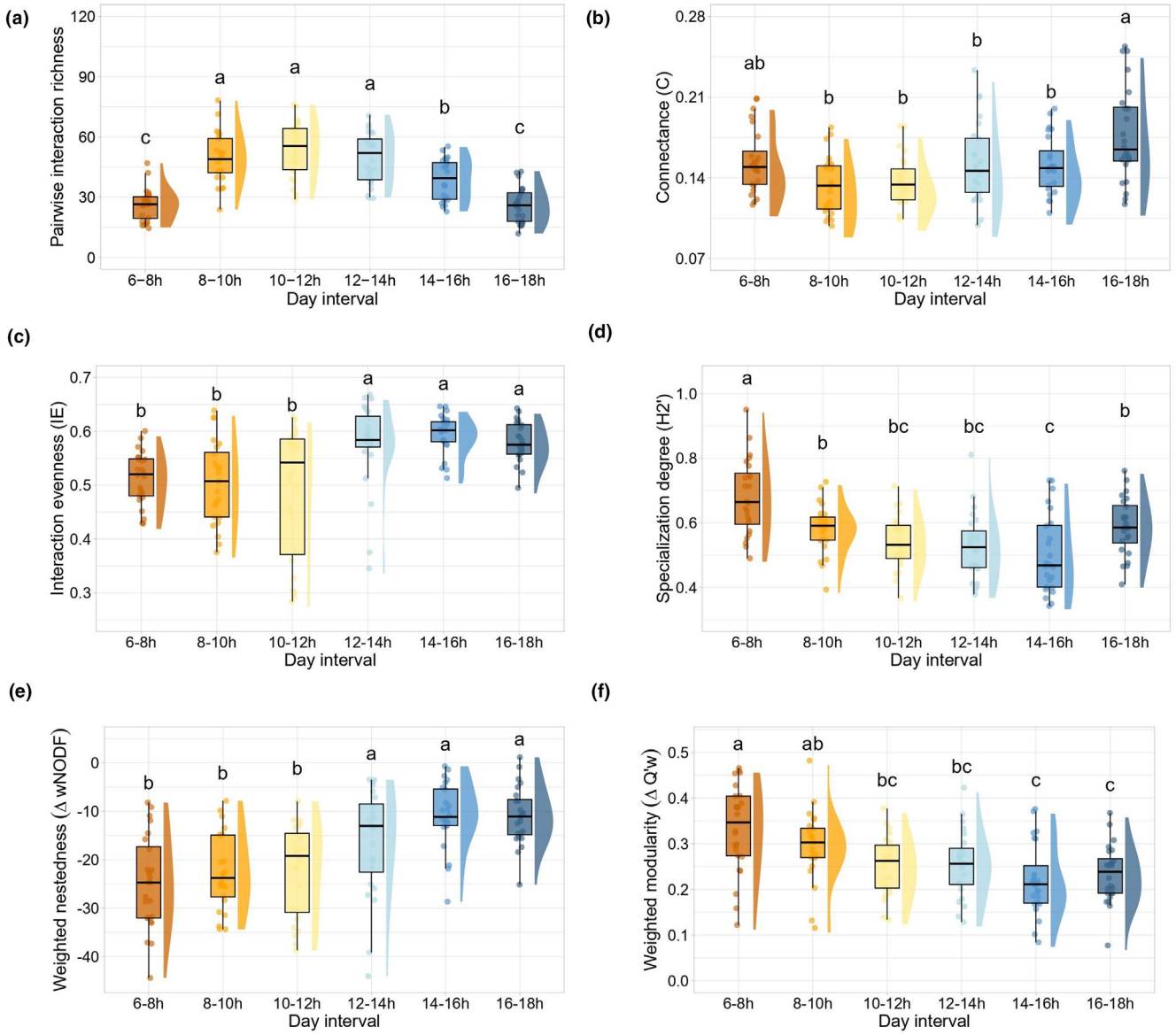

FIGURE 1 Network structure across daily sampling periods. Points depict the score of weighted network metrics extracted for each 2-h sampling period in each plot and flowering season ($n=24$ scores for each sampling period). Sampling periods occupying a central position within the day demonstrate consistently higher levels of pairwise interaction richness (a), but lower levels of connectance (b). From early morning to late-afternoon (i.e. the orange-blue continuum) networks exhibit progressively higher levels of interaction evenness (c) and nestedness (e), but lower levels of network specialisation (d) and compartmentalisation (f). Compact letter displays highlight significant differences in network metric scores following Tukey *post hoc* analyses.

Plant–bee interaction β-diversity (i.e. β^{WN}) was very different among sampling periods ($\chi^2_{14,346}=488.62$; $R^2_{adjusted}=0.98$; $p<0.01$). Notably, plant–bee interaction dissimilarity increased consistently with increasing temporal distance between sampling periods (Figure 2a). Furthermore, the lowest interaction β-diversity occurred during sampling periods around midday (Figure 2a). Plant–bee interaction β-diversity was driven more by interaction rewiring between shared species (i.e. β^{OS}) than by the species turnover (i.e. β^{ST}; Figure 2b).

3.2 | Assessing the structural and compositional representativeness of partial-day networks

Increasing the number of sampling periods enhanced the potential for sampling a broader range of occurring plant–bee interactions. However, the ability of partial-day networks to resemble the full-day network in terms of structure varied across different combinations of sampling periods (Figure 3). While the pairwise interaction richness, *C*, *H2′*, *wNODF* and *Qw′* became more similar to the full-day network following progressive additions of 2-h sampling periods (Figure 3a,b,d–f), *IE* did not follow the same trend (Figure 3c). Moreover, especially for interaction richness, *H2′*, *wNODF*, *Qw′*, the added value of sampling interaction around midday (i.e. from 08:00–10:00 to 12:00–14:00) was greater than focusing on sampling the extremes of the day (i.e. 06:00–8:00 and 16:00–18:00). This sampling interval alone accounts for 82.0% of all recorded interactions and 79.7% of all unique pairwise interactions (Table 1). In general, combinations of four 2-h sampling periods, particularly from 08:00–10:00 to 14:00–16:00, were sufficient to capture network topology comparable to that obtained from continuous daylight monitoring. Despite that, covering the earliest and latest sampling period (i.e. 06:00–08:00 and 16:00–18:00)

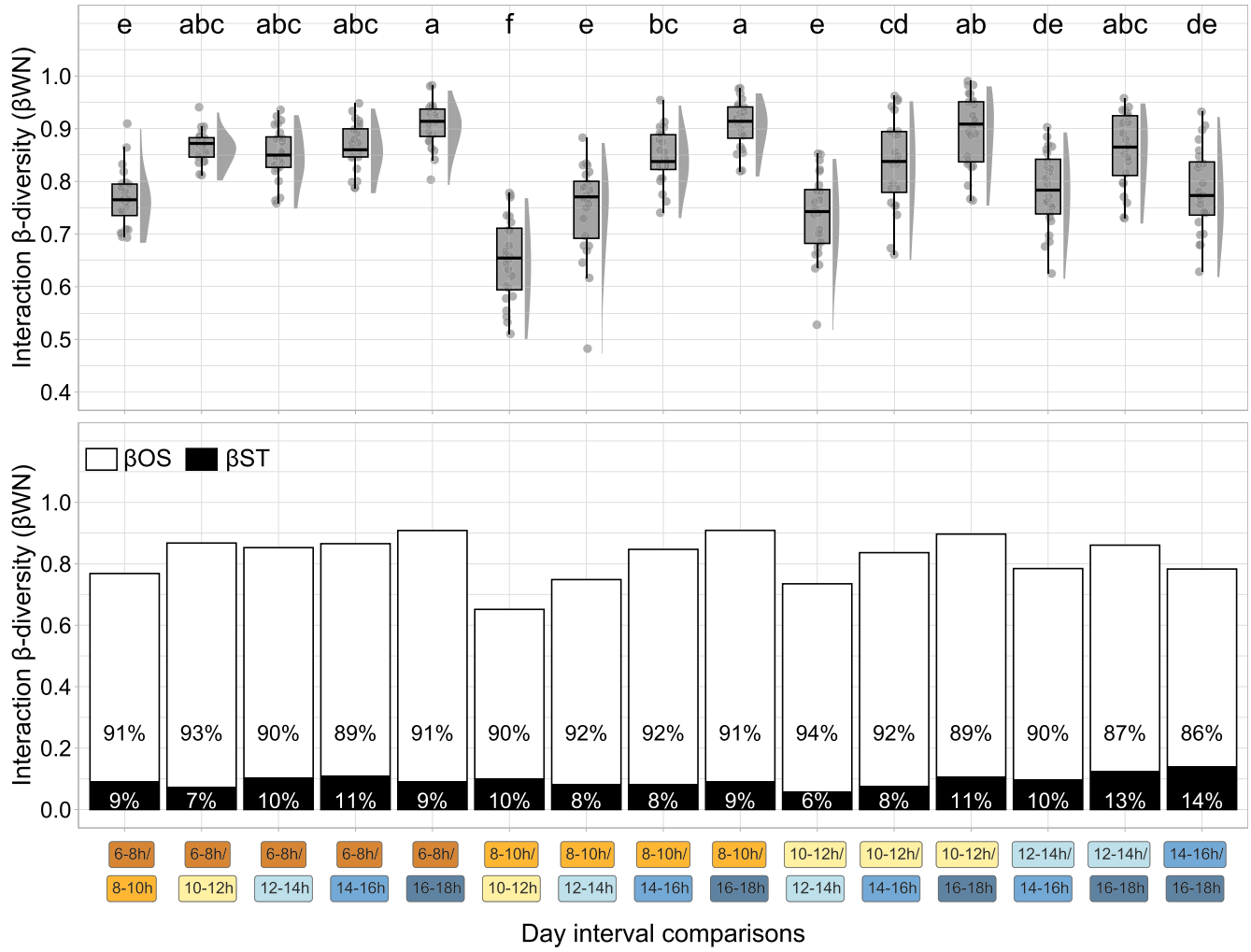

FIGURE 2 Interaction β-diversity across daily sampling periods. Points represent pairwise comparisons among 2-h sampling periods within the same plot and flowering season ($n=24$ comparisons for each pair of sampling periods). Each boxplot represents one of all the possible comparisons between pairs of distinct sampling periods. Differences in overall interaction β-diversity (i.e. β^{WN}; a) increase with an extended time interval between compared sampling periods. Interaction rewiring (i.e. βOS; in white; b) is often more important than species turnover (β^{ST}; in black; b) to explain the overall interaction β-diversity. β^{ST} generally remains stable across comparisons of sampling periods but shows the lowest values when comparing periods occurring in the central hours of the day (e.g. 10-12 h and 12-14 h).

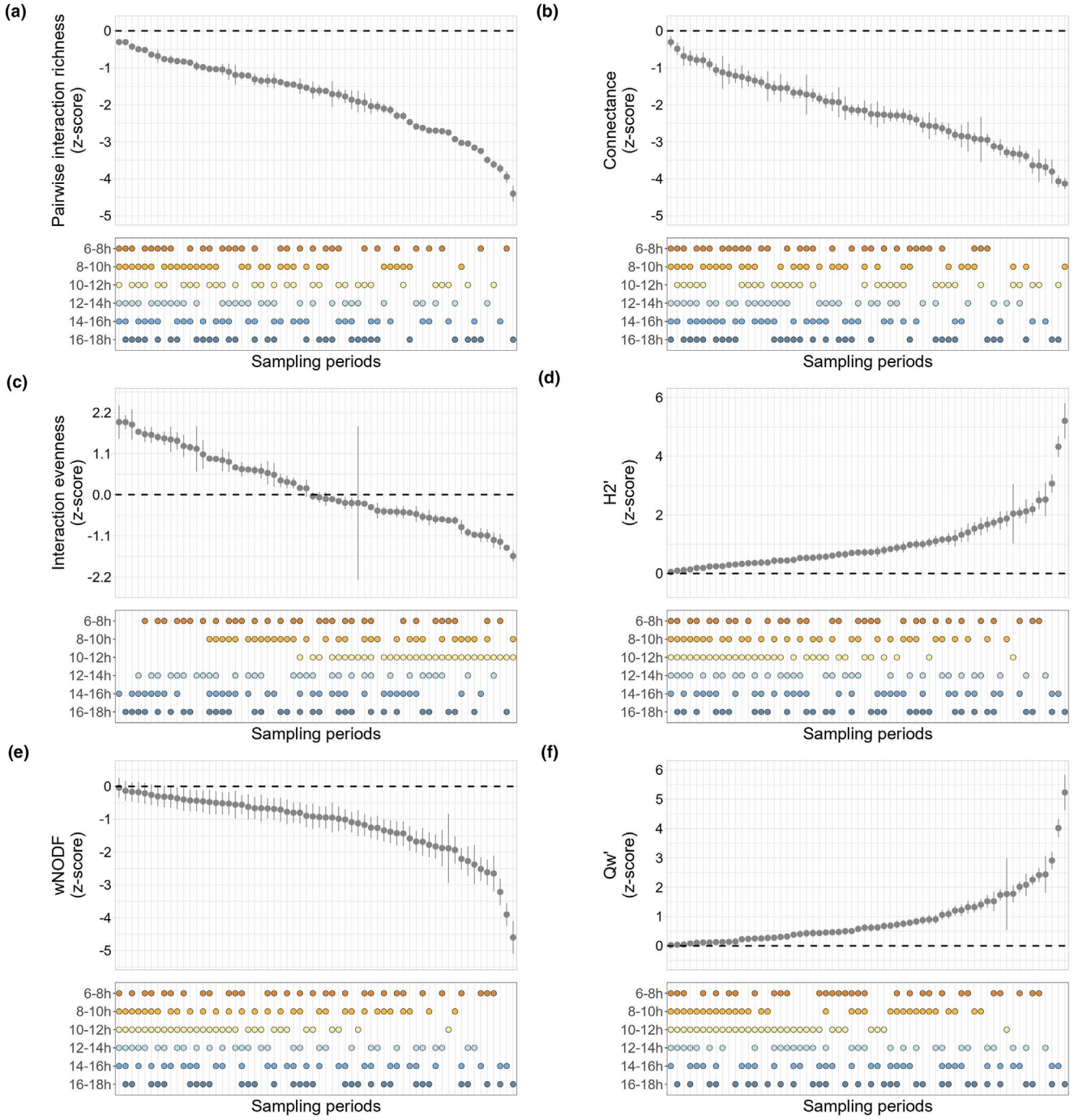

FIGURE 3 Optimal sampling periods resembling the full-day network across 2-h sampling combinations. Point ranges depict z-score values obtained from null matrices for particular partial-day networks (mean ± SD). Each panel contains 62 point ranges representing each partial-day network. Partial-day networks closer to the horizontal dashed line represent those that mostly align with the values of a specific network metric observed in the full-day network. Circles below the graph are coloured following the orange-blue continuum (6-8 h: dark orange; 16–18 h: dark blue) and ordered according to the number of sampling periods that were merged to build the network.

enhanced pairwise interaction richness, contributing to the completeness of recorded interactions.

Interaction composition dissimilarities (β^{WN}) between the full- and the partial-day networks generally decreased as additional 2-h sampling periods were included (Figure 4). The best combinations for one to five periods showed a monotonic decrease in β^{WN}, from a single central period (08:00–10:00; $\beta^{WN} \approx 0.75$), to two (08:00–12:00; ≈0.45), three (08:00–14:00; ≈0.27), four (06:00–14:00; ≈0.15), and five periods (06:00–16:00; ≈0.05). Accordingly, combinations covering the central hours of the day (i.e. 08:00–14:00) consistently yielded partial-day networks more similar to the full-day network, outperforming other combinations with the same or even greater sampling effort that did not fully cover this central window (Figure 4). Additionally, sampling during

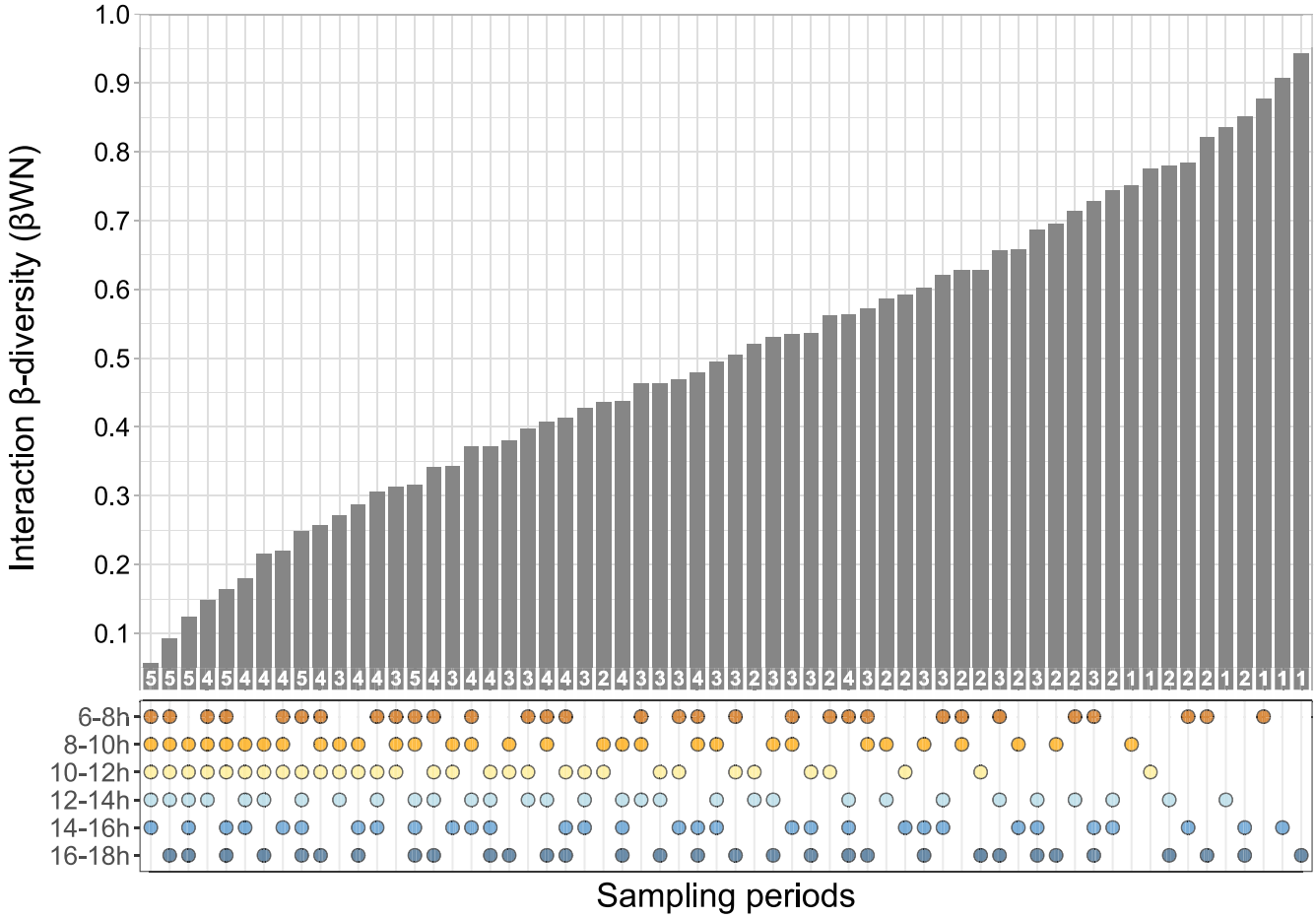

FIGURE 4 Plant–bee interaction β-diversity among each partial- and the full-day network. The bar plots represent the mean value of the overall β-diversity of plant–bee interactions (i.e. β^{WN}) among each partial-day network and the full-day network. Each bar corresponds to a partial-day network, indicating which sampling periods were combined to create the interaction matrix. Circles below the graph are coloured following the orange-blue continuum (6–8 h: dark orange; 16–18 h: dark blue) and ordered according to the number of sampling periods that were merged to build the network. The numbers within each bar denote the number of sampling periods that were merged.

the earliest period of the day proved to be more informative than sampling near dusk (Figure 4).

Together, these results indicate that central daytime periods recover interaction composition close to the full-day network, driving similarity in weighted metrics and overall network structure, whereas early-morning and late-afternoon intervals capture additional, presumably rare interactions.

3.3 | Identifying network metrics less sensitive to varying sampling effort

The full-day network was non-nested, presented low connectance and exhibited moderate levels of specialisation and modularity (Figure 5). Although partial-day networks increasingly resembled the full-day network as more 2-h periods were added, their topological properties still varied substantially with sampling effort (Figure 5). Following the addition of 2-h sampling periods, pairwise interaction richness, connectance (*C*) and nestedness (*wNODF*) increased in both simulated and empirical networks (Figure 5a,b,e). Conversely, network specialisation (*H2′*) and modularity (*Qw′*) decreased in simulated networks but stabilised at intermediate values in empirical ones as sampling increased (Figure 5d,f). Interaction evenness (*IE*), in turn, became less variable and converged to intermediate values in both null and empirical networks (Figure 5c).

The number of merged sampling periods influenced all studied network metrics (Figure 5). Pairwise interaction richness tended to be higher in null networks (Figure 5a). Furthermore, differences between null and empirical networks were evident across all sampling periods. Notably, *C*, *H2′*, *wNODF* and *Qw′* differed significantly from randomised networks even under minimal sampling (i.e. single 2-h periods; Figure 5b,d–f). For *IE*, at least four 2-h sampling periods were required to achieve significant scores in empirical networks (Figure 5c).

3.4 | Intra- and inter-seasonal consistency of daily interaction patterns

Interaction frequency and pairwise interaction richness varied across weeks, phenological blocks and flowering seasons, but their

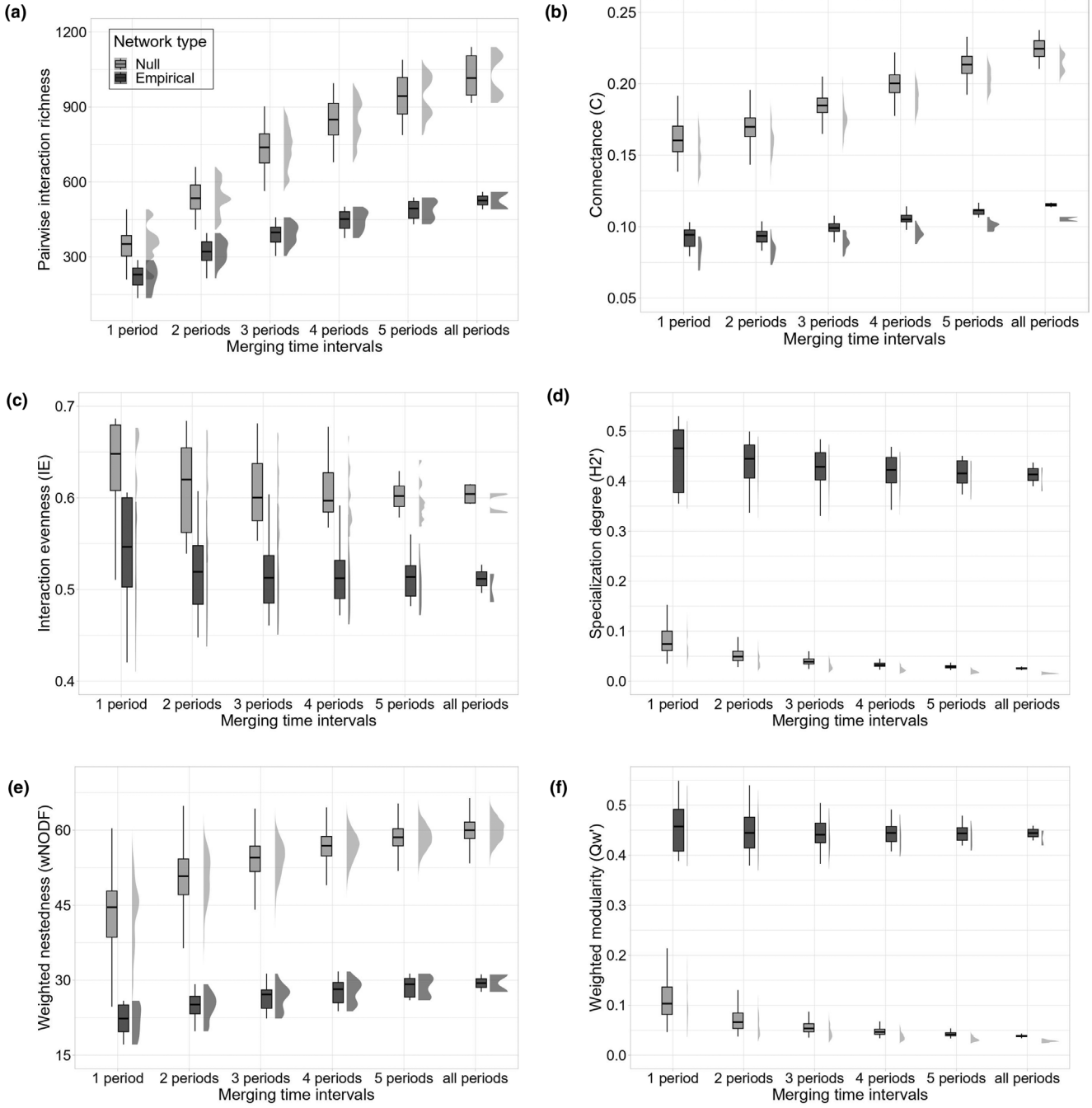

FIGURE 5 Projection of the network metrics extracted for null matrices for each partial- and full-day network. In each graph, from the left to the right, boxplots illustrate the empirical (dark grey) or the expected (light grey) network metric scores for networks polling data on plant–bee interactions over one to six 2-h sampling periods (i.e. the full-day network). There is generally less variation in network metrics as the number of 2-h sampling periods increases. While pairwise interaction richness (a), connectance (b) and network nestedness (e) tend to increase following the inclusion of additional daily sampling periods, the degree of network-wide specialisation (d) and network modularity (f) tends to decrease. Intermediate scores of interaction evenness (c) are achieved with the addition of more 2-h sampling periods. Non-overlapping dark and light grey boxplots in each sampling period indicate that results from the empirical network are likely biologically meaningful (i.e. not obtained by chance).

relative distribution among 2-h sampling periods remained consistent (Figures S3 and S4). Likewise, differences in network structure among periods were stable within and between flowering seasons (Figures S5 and S10), with only minor deviations during the early-season block. Interaction dissimilarity also consistently increased with temporal distance between periods across phenological blocks (Figure S11; Tables S3 and S4). Similarly, assessments of partial-day network representativeness were consistent across seasons and phenological blocks (Figure S12), with midday periods showing the lowest dissimilarity relative to full-day networks. Thus, although seasonal phenological turnover affected overall interaction magnitude, it did not explain differences among 2-h daily sampling periods.

4 | DISCUSSION

Empirically sampled ecological interaction inventories, as any result of a sampling protocol, often exhibit a subset of the actual pairwise species-species interactions occurring in nature (Chacoff et al., 2012; Jordano, 2016). One of the reasons for such limitation arises from selecting a specific temporal window that can capture the fraction of interactions only occurring within that timeframe. However, it is common to extrapolate observed patterns of ecological interactions from a specific temporal window to infer underlying processes encompassing interactions in unsampled windows. For instance, many recent studies worldwide have focused on sampling plant–bee interactions during specific daylight hours to optimise effort and cost while maximising interaction records (see Hachuy-Filho et al., 2020; Burkle et al., 2022 as examples). However, they might implicitly assume that the findings from this limited timeframe reflect patterns across the entire daylight period. In this study, we demonstrate that sampling plant–bee interactions at different times throughout the day leads to considerable variability in plant–bee network composition and structure. Through this method-directed analysis, we demonstrate that strategically balancing sampling efforts across different periods of the day ensures datasets of plant–bee interactions capable of reliably reflecting the structure and properties of full-day sampled networks. The full-day network was used as a benchmark because it represents the most complete approximation of plant–bee interactions occurring within the daylight activity window, which is the relevant temporal scale over which these interactions take place.

Our results show that restricting sampling to specific portions of the day captures dominant interaction patterns but misses many unique and rare interactions, altering both network composition and inferred structure. This has important implications for ecological inference, as studies comparing network structure across ecological gradients (e.g. latitude, elevation or habitat type) may attribute differences in metrics, such as specialisation or nestedness, to environmental drivers when they instead reflect differences in daily sampling windows. By comparing partial-day networks to a full-day benchmark, our approach provides a more robust assessment of how restricted temporal sampling may bias inferences about ecological network structure and composition. Thus, similarly to studies showing that time-sensitive sampling must be accounted for at broader temporal scales (e.g. CaraDonna et al., 2021; Olesen et al., 2010; Schwarz et al., 2020), our results demonstrate that sampling only part of the day may not reliably represent daily interactions, with consequences for the representation of network structure.

4.1 | Composition and structure of empirical networks across sampling periods within the day

Network structure varied consistently among sampling periods within the day. Specialisation and modularity were higher in early-morning periods, whereas nestedness and interaction evenness increased after midday. Interaction richness and frequency peaked during midday periods, with lower values observed at the beginning and end of the day. This pattern suggests a shift from more modular and specialised interaction sets in the early morning to more generalised and hierarchically organised patterns later in the day. The higher connectance near dusk is consistent with fewer plant species remaining in bloom, forcing pollinators to concentrate on a reduced set of resources and generating a denser web of interactions. Accordingly, the species-turnover component explained a larger yet still minor fraction of overall β-diversity near dusk, likely due to flower closure in some plant species. These findings imply that resource utilisation patterns undergo significant changes from dawn to dusk, primarily due to the rewiring of interactions, albeit influenced to some degree by species turnover within the day (Ratoni et al., 2025; but see Nagano, 2023). The dynamical rewiring of interactions throughout the day and the strong contribution of interaction richness and frequency around midday periods are likely to play a key role in shaping the daily structural variation of plant–bee ecological networks.

Plant and bee life-history traits shape interaction patterns across the day. On the plant side, flowering phenology and resource availability strongly influence pollinator use (Baldock et al., 2011; Herrera, 1990). Some species open or close flowers at specific times, creating forbidden links for pollinators active outside those periods (Fründ et al., 2011), boosting interaction turnover. Moreover, flowers often show daily peaks in nectar production and pollen presentation, prompting shifts in foraging strategies and rewiring interactions among visitors (Ballarin et al., 2022; Štenc et al., 2023). On the bee side, foraging activity varies among species according to morphological and physiological traits that mediate responses to wind, temperature and light (Herrera, 1990, 2024; Polatto et al., 2014; Willmer & Stone, 2004), driving interaction turnover. Moreover, changes in floral availability at fine temporal scales lead bees to adjust their foraging, increasing interaction rewiring (Herrera, 1990; Polatto et al., 2014; Nagano, 2023; Arrowsmith et al., 2025; Arroyo-Correa, 2025). Such temporal dynamics in floral availability help explain why specialisation and modularity are higher in the early morning, when interactions are dominated by large-bodied and more specialised bees (e.g. *Centris* and *Epicharis*; see Table S1) that tolerate milder climatic conditions and often concentrate their foraging on a single plant species offering resources of restricted use (e.g. oil). As the day progresses towards midday, the increasing number of simultaneously open flowers expands resource availability, reducing specialisation and gradually increasing nestedness as interactions become structured by a more hierarchical and competitive use of resources. Later in the day, flower closure and resource depletion further reduce resource availability, leading to higher connectance and interaction evenness, and reinforcing nestedness. Thus, the timing of flower opening, the dynamics of floral reward availability and diel patterns of bee activity likely modulate visitation to co-flowering plants and shape network structure throughout the day.

All this suggests that early-morning periods disproportionately capture interactions involving more specialised species and well-defined modules, whereas midday and late-day networks increasingly reflect the activity of generalist species and the progressive

concentration of interactions on fewer floral resources. Consequently, the time-of-day emphasised in empirical studies will shape which facets of network organisation are most clearly expressed, from specialised and modular structures to the broader structure of resource competition.

These temporal shifts in interaction structure have important implications for conservation and ecological inference. Temporally restricted sampling may overrepresent interactions dominating specific periods while underrepresenting those contributing to network structure at other times. Consequently, estimates of connectivity, nestedness or interaction distribution may reflect the sampling window rather than the integrated diurnal structure of the network. This bias can also affect conservation prioritisation by emphasising taxa or links disproportionately represented during peak sampling periods (Ballarin et al., 2024; Ulrich & Peters, 2023) while overlooking interactions important in other daily windows. In systems where interaction structure varies across the day, this may lead to incomplete representations of network organisation and suboptimal conservation decisions.

4.2 | Assessing the structural and compositional representativeness of partial-day networks

Beyond documenting daily changes in empirical plant–bee interaction networks, our chronologically structured sampling protocol allowed us to evaluate how different combinations of 2-h periods perform in reconstructing network structure under realistic sampling schedules. Although sampling throughout the entire day provides the most complete description of the system (Baldock et al., 2011), logistic and funding limitations often make this unfeasible in practice (Hegland et al., 2010).

Our results show that strategically combining daily sampling windows can efficiently approximate full-day network structure. Networks assembled from four 2-h periods consistently achieved low interaction turnover (β^{WN} <0.2) relative to the full-day network, while recovering up to ~80% of all pairwise interactions and ~82% of interaction frequencies. Combinations dominated by central daytime hours maximised interaction richness and, critically, reproduced interaction frequencies close to those of the full-day network, which explains their high resemblance in weighted network metrics. This reflects the peak of bee activity, when most bee-pollinated plants are simultaneously open and rewarding (Nagano, 2023). In contrast, early-morning and late-afternoon periods, although contributing fewer interactions, add a disproportionate number of unique links, presumably rarer and temporally restricted, thereby enriching the pool of recorded pairwise interactions.

Still, sampling design and metric choice should be aligned with study goals. If the objective is to characterise network structure, interaction asymmetries or identify core species involved in frequent interactions, central daytime windows are most efficient; if the goal is to maximise interaction diversity, detect specialised or rare links and better resolve modular structure, distributing sampling across the day, especially including early-morning periods, is likely ideal, as it introduces interactions absent from other periods but frequent enough to influence network structure.

4.3 | Identifying network metrics less sensitive to varying sampling effort

Frequency-based network metrics consistently captured network structure and showed predictable trends with the addition of sampling periods (Vizentin-Bugoni et al., 2016). While *IE* and interaction richness exhibited higher variability across combinations, *H2′*, *wNODF* and *Qw′* converged rapidly towards full-day values when sampling was concentrated in the central daylight hours. Overall, increased sampling effort increased nestedness and connectance, whereas intermediate levels of specialisation and modularity emerged as periods were added. Importantly, empirical values of *C*, *H2′*, *wNODF* and *Qw′* consistently departed from null expectations, indicating that these metrics capture biologically structured patterns even under temporally restricted sampling.

Our results show that network metrics differ in their sensitivity to restricted temporal sampling. Under limited sampling windows, weighted metrics provide more reliable and stable estimates of network structure, especially when sampling is concentrated in periods that accumulate higher interaction richness and frequencies. This is because metrics, such as *H2′*, *wNODF*, *Qw′* and *C* readily depart from null expectations and show comparatively smaller variation as additional sampling periods are added. In contrast, pairwise interaction richness and interaction evenness are more sensitive to sampling effort and only stabilise and consistently depart from null models after a larger fraction of the day has been sampled. Therefore, when temporal coverage is necessarily restricted, weighted metrics are more appropriate for structural inference, whereas characterising the full pool and diversity of interactions requires distributing sampling effort across the day.

4.4 | Intra- and inter-seasonal consistency of daily interaction patterns

Although temporal variation in plant–pollinator network structure across the flowering season is well documented (e.g. Alarcón et al., 2008; Ballarin, Amorim, et al. 2026; Ballarin, Fidelis, et al., 2026; CaraDonna et al., 2017; Resasco et al., 2021), our results show that intra-daily variation is also a consistent component of network organisation. Some reduction in this consistency occurs early in the season, when lower species richness and cooler temperatures increase variability in interactions and amplify short-term ecological constraints. Despite this, the overall diel signature remains detectable across the season, reinforcing that daily processes are embedded within seasonal dynamics. Consequently, intra-daily variation should be explicitly considered in network studies, as broader-scale patterns attributed to seasonal or interannual processes may partly reflect differences in sampling time-of-day. This has direct implications for cross-study comparisons, particularly when networks are

sampled across different flowering periods without standardised daily sampling windows, potentially confounding temporal scales in inferred network structure.

4.5 | A general framework for daily sampling of time-sensitive interactions

While increasing sampling effort is time- and labour-intensive, monitoring ecological interactions is increasingly critical in systems undergoing rapid environmental change (Jordano, 2016). Here, rather than proposing a universal protocol, we outline a general framework to evaluate how the choice of daily sampling windows affects the representativeness of interaction networks (Figure 6). The main idea is that missing interactions are not necessarily recovered by increasing effort within a restricted time window, but often by expanding or repositioning the sampling window itself.

The approach consists of conducting pilot samplings across the main daily windows of activity, building time-specific networks, and then combining them to generate partial- and full-day networks (Hegland et al., 2010). Partial-day networks can then be evaluated according to how well they approximate the full-day network in terms of structure and interaction configuration, and network metrics can be screened for their sensitivity to incomplete temporal coverage (Vizentin-Bugoni et al., 2016). This allows researchers to identify (i) the minimum effort needed to obtain a representative network, (ii) how this effort should be distributed across the day, and (iii) which descriptors are more robust to temporal subsampling. For example, when full-day sampling is

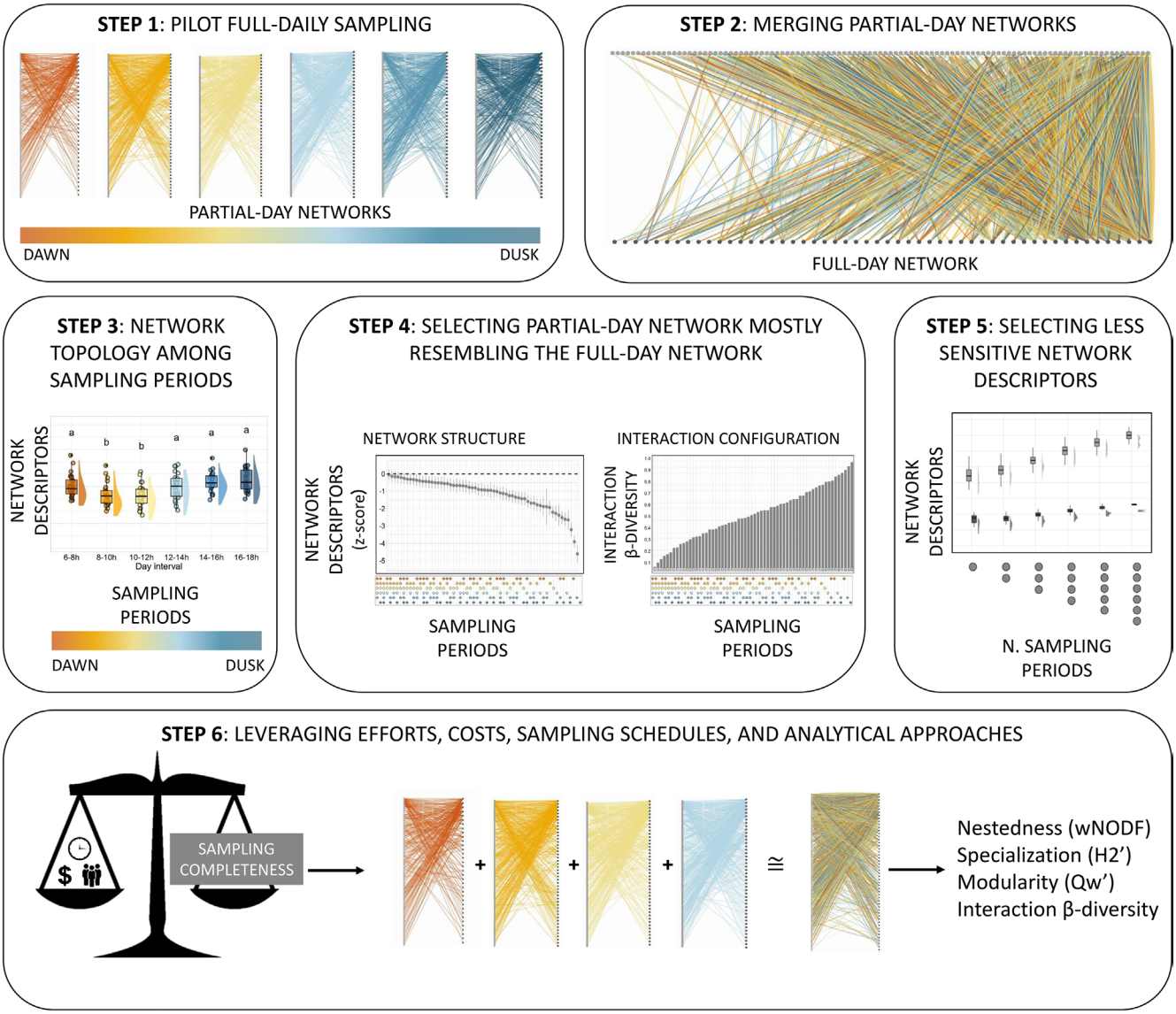

FIGURE 6 Framework for the daily sampling of plant–bee interaction networks. A step-by-step routine is suggested to inspect whether the structure and configuration of plant–bee interaction networks vary throughout the day and to determine the best combination of sampling periods to build partial-day networks closely resembling the full-day network.

unfeasible due to long daylight periods or logistical constraints, the day can be divided into discrete time slices to identify combinations that best approximate the full-day network.

Importantly, the most informative sampling window will be context-dependent. Systems may differ markedly in their diel dynamics, and, in some cases, sampling during the periods of highest interaction activity will disproportionately increase network representativeness, likely because these periods concentrate not only interaction frequency but also interacting species richness. In other ecological contexts (e.g. temperate or species-poor systems), plant–pollinator diel dynamics may follow different patterns. Nevertheless, even in such cases, the daily interaction window can still be partitioned into meaningful intervals tailored to identify the most informative periods. Although our discussion is framed around plant–bee interactions, the same logic applies whenever interactions are structured in temporal or spatial slices (e.g. plots, months, seasons or years) and is particularly relevant for conservation-oriented studies and comparative syntheses that implicitly assume that a locally sampled network is representative of the underlying interaction system.

5 | CONCLUSION

Daily changes in pairwise plant–bee interactions have a significant signal in plant–bee network structure, which implies that different sampling schedules may yield different, somehow biased, network properties. Still, we demonstrate that employing a comprehensive sampling design that encompasses the period of higher plant availability and bee activity might yield results resembling a network covering the entire daylight span. Although sampling plant–bee interactions spanning all the day might be demanding, future studies should (i) draw sampling schedules aiming to track daily variations in plant–bee pairwise interactions or (ii) explicitly recognise that results coming from limited sampling periods should ideally not be extrapolated to broader temporal daily windows, as networks built in different daily timeframes may manifest significant topological disparities.

AUTHOR CONTRIBUTIONS

Caio S. Ballarin and Jorge Isla conceived the ideas. Caio S. Ballarin designed the methodology. Caio S. Ballarin and Leandro Hachuy-Filho collected the data. Caio S. Ballarin, Jorge Isla, Elena Quintero, Blanca Arroyo-Correa and Pedro Jordano analysed the data and validated the results. Caio S. Ballarin led the writing of the manuscript. All authors contributed critically to the drafts and gave final approval for publication.

ACKNOWLEDGEMENTS

We thank all colleagues at the Laboratório de Ecologia da Polinização e Interações (LEPI) for their assistance during the fieldwork. We also express our gratitude to the colleagues at the BOTU herbarium, and to Eduardo Almeida for helping us identify the plant and bee species, respectively. We thank André Simões Ballarin for his invaluable assistance with data curation. The Fundação Coordenação de Aperfeiçoamento de Pessoal de Nível Superior (CAPES—Finance Code 001; CAPES PrInt—grant number: 88887.839479/2023-00) supported CSB's PhD study and his PhD sandwich. FWA and CSB are associated with the Center for Research on Biodiversity Dynamics and Climate Change (CEPID FAPESP no. 2021/10639-5; CSB Postdoctoral Research grant number: 2024/02640-1). The Article Processing Charge for the publication of this research was funded by the Coordenação de Aperfeiçoamento de Pessoal de Nível Superior - Brasil (CAPES) (ROR identifier: 00x0ma614).

CONFLICT OF INTEREST STATEMENT

There is no conflict of interest to disclose.

Our study brings together authors from two different countries (and continents), including scientists based in the country where the study was carried out. Whenever relevant, literature published by scientists from the region was cited; efforts were made to consider relevant work published in the local language.

DATA AVAILABILITY STATEMENT

Data are available from the Figshare Repository: https://doi.org/10.6084/m9.figshare.32744535 (S. Ballarin, Isla, et al., 2026).

ORCID

Caio S. Ballarin https://orcid.org/0000-0001-8299-3189
Jorge Isla https://orcid.org/0000-0002-2307-9730
Blanca Arroyo-Correa https://orcid.org/0000-0002-9402-3013
Elena Quintero https://orcid.org/0000-0003-4979-6874
Felipe W. Amorim https://orcid.org/0000-0002-6026-0395
Pedro Jordano https://orcid.org/0000-0003-2142-9116

REFERENCES

Alarcón, R., Waser, N. M., & Ollerton, J. (2008). Year-to-year variation in the topology of a plant–pollinator interaction network. *Oikos*, *117*(12), 1796–1807.

Arrowsmith, K. C., Strait, M. D., Chandar, M., Schiffer, A., & Brosi, B. J. (2025). Temperature influences pollinators' choice of floral partners independently of community composition. *Journal of Animal Ecology*, *00*, 1–13. https://doi.org/10.1111/1365-2656.70158

Arroyo-Correa, B. (2025). When temperature calls the shots: Pollinators' floral choices in a warming world. *Journal of Animal Ecology*, *00*, 1–4. https://doi.org/10.1111/1365-2656.70149

Arroyo-Correa, B., Burkle, L. A., & Emer, C. (2020). Alien plants and flower visitors disrupt the seasonal dynamics of mutualistic networks. *Journal of Ecology*, *108*(4), 1475–1486.

Baldock, K. C., Memmott, J., Ruiz-Guajardo, J. C., Roze, D., & Stone, G. N. (2011). Daily temporal structure in African savanna flower visitation networks and consequences for network sampling. *Ecology*, *92*(3), 687–698.

Ballarin, C. S., Amorim, F. W., Arroyo-Correa, B., & Jordano, P. (2026). Floral resource diversity drives spatiotemporal variation in plant–pollinator network structure. *Oikos*, *2026*, e11730. https://doi.org/10.1002/oik.11730

Ballarin, C. S., Amorim, F. W., Watson, D. M., & Fontúrbel, F. E. (2024). The use and abuse of keystone plant species in restoration practices of terrestrial ecosystems. *Restoration Ecology*, *32*(1), e14030.

Ballarin, C. S., Fidelis, A., Maruyama, P. K., & Amorim, F. W. (2026). Fire-driven fine-scale diversity of Cerrado flowering plants and their bee pollinators in space and time. *Annals of Botany*, mcag033. https://doi.org/10.1093/aob/mcag033

Ballarin, C. S., Hachuy-Filho, L., Doria, M. J. W., Giffu, M. M., Polizello, D. S., Oliveira, P. H., Lacerda-Barbosa, P. A., & Amorim, F. W. (2022). Intra-seasonal and daily variations in nectar availability affect bee assemblage in a monodominant afforested Brazilian Cerrado. *Austral Ecology*, *47*(6), 1315–1328.

Ballarin, C. S., Isla, J., Arroyo-Correa, B., Quintero, E., Hachuy-Filho, L., Amorim, F. W., & Jordano, P. (2026). Data from: "Optimising daily sampling of plant–bee interaction networks". Figshare repository. https://doi.org/10.6084/m9.figshare.32744535

Ballarin, C. S., Lacerda-Barbosa, P. A., Moraes, A. P., Campos, F. G., & Amorim, F. W. (2025). From bats to bees: Changes in flower anthesis and nectar traits drive a pollination ecotype in dwarf *Caryocar brasiliense* (Caryocaraceae). *Annals of Botany*, mcaf263. https://doi.org/10.1093/aob/mcaf263

Basilio, A. M., Medan, D., Torretta, J. P., & Bartoloni, N. J. (2006). A year-long plant-pollinator network. *Austral Ecology*, *31*(8), 975–983.

Beckett, S. J. (2016). Improved community detection in weighted bipartite networks. *Royal Society Open Science*, *3*(1), 140536.

Blüthgen, N., Menzel, F., & Blüthgen, N. (2006). Measuring specialisation in species interaction networks. *BMC Ecology*, *6*(1), 1–12.

Bramon Mora, B., Shin, E., CaraDonna, P. J., & Stouffer, D. B. (2020). Untangling the seasonal dynamics of plant–pollinator communities. *Nature Communications*, *11*(1), 4086.

Burkle, L. A., Belote, R. T., & Myers, J. A. (2022). Wildfire severity alters drivers of interaction beta-diversity in plant–bee networks. *Ecography*, *2022*(3), e05986.

CaraDonna, P. J., Burkle, L. A., Schwarz, B., Resasco, J., Knight, T. M., Benadi, G., Blüthgen, N., Dormann, C. F., Fang, Q., Fründ, J., Gauzens, B., Kaiser-Bunbury, C. N., Winfree, R., & Vázquez, D. P. (2021). Seeing through the static: The temporal dimension of plant–animal mutualistic interactions. *Ecology Letters*, *24*(1), 149–161.

CaraDonna, P. J., Petry, W. K., Brennan, R. M., Cunningham, J. L., Bronstein, J. L., Waser, N. M., & Sanders, N. J. (2017). Interaction rewiring and the rapid turnover of plant–pollinator networks. *Ecology Letters*, *20*(3), 385–394.

CaraDonna, P. J., & Waser, N. M. (2020). Temporal flexibility in the structure of plant–pollinator interaction networks. *Oikos*, *129*(9), 1369–1380.

Chacoff, N. P., Vázquez, D. P., Lomáscolo, S. B., Stevani, E. L., Dorado, J., & Padrón, B. (2012). Evaluating sampling completeness in a desert plant–pollinator network. *Journal of Animal Ecology*, *81*(1), 190–200.

Chao, A. (1984). Nonparametric estimation of the number of classes in a population. *Scandinavian Journal of Statistics*, *11*, 265–270.

Dorado, J., Vázquez, D. P., Stevani, E. L., & Chacoff, N. P. (2011). Rareness and specialisation in plant–pollinator networks. *Ecology*, *92*(1), 19–25.

Dormann, C. F., Gruber, B., & Fründ, J. (2008). Introducing the bipartite package: Analysing ecological networks. *R News*, *8*, 8–11.

Fründ, J., Dormann, C. F., & Tscharntke, T. (2011). Linné's floral clock is slow without pollinators–flower closure and plant-pollinator interaction webs. *Ecology Letters*, *14*(9), 896–904.

Fründ, J., McCann, K. S., & Williams, N. M. (2016). Sampling bias is a challenge for quantifying specialisation and network structure: Lessons from a quantitative niche model. *Oikos*, *125*(4), 502–513.

Gotelli, N. J., & Colwell, R. K. (2011). Estimating species richness. In A. E. Magurran & B. J. McGill (Eds.), *Biological diversity frontiers in measurement and assessment* (pp. 39–54). Oxford University Press.

Hachuy-Filho, L., Ballarin, C. S., & Amorim, F. W. (2020). Changes in plant community structure and decrease in floral resource availability lead to a high temporal β-diversity of plant–bee interactions. *Arthropod-Plant Interactions*, *14*(5), 571–583.

Hegland, S. J., Dunne, J., Nielsen, A., & Memmott, J. (2010). How to monitor ecological communities cost-efficiently: The example of plant–pollinator networks. *Biological Conservation*, *143*(9), 2092–2101.

Herrera, C. M. (1990). Daily patterns of pollinator activity, differential pollinating effectiveness, and floral resource availability, in a summer-flowering Mediterranean shrub. *Oikos*, *58*(3), 277–288.

Herrera, C. M. (2024). Thermal biology diversity of bee pollinators: Taxonomic, phylogenetic, and plant community-level correlates. *Ecological Monographs*, *94*, e1625.

Hsieh, T. C., Ma, K. H., & Chao, A. (2016). iNEXT: An R package for rarefaction and extrapolation of species diversity (hill numbers). *Methods in Ecology and Evolution*, *7*(12), 1451–1456.

Jordano, P. (2016). Sampling networks of ecological interactions. *Functional Ecology*, *30*(12), 1883–1893.

Lenth, R. V. (2016). Least-squares means: The R package lsmeans. *Journal of Statistical Software*, *69*, 1–33.

Levin, S. A. (1992). The problem of pattern and scale in ecology: The Robert H. MacArthur award lecture. *Ecology*, *73*(6), 1943–1967.

Magrach, A., González-Varo, J. P., Boiffier, M., Vilà, M., & Bartomeus, I. (2017). Honeybee spillover reshuffles pollinator diets and affects plant reproductive success. *Nature Ecology & Evolution*, *1*(9), 1299–1307.

Magurran, A. E. (1988). *Ecological diversity and its measurement*. Springer Science & Business Media.

Nagano, Y. (2023). Changes in pollinators' flower visits and activities potentially drive a diurnal turnover of plant-pollinator interactions. *Ecological Entomology*, *48*(6), 650–657.

Olesen, J. M., Bascompte, J., Dupont, Y. L., Elberling, H., Rasmussen, C., & Jordano, P. (2011). Missing and forbidden links in mutualistic networks. *Proceedings of the Royal Society B: Biological Sciences*, *278*(1706), 725–732.

Olesen, J. M., Bascompte, J., Dupont, Y. L., & Jordano, P. (2007). The modularity of pollination networks. *Proceedings of the National Academy of Sciences*, *104*(50), 19891–19896.

Olesen, J. M., Bascompte, J., Elberling, H., & Jordano, P. (2008). Temporal dynamics in a pollination network. *Ecology*, *89*(6), 1573–1582.

Olesen, J. M., Dupont, Y. L., O'Gorman, E., Ings, T. C., Layer, K., Melian, C. J., Trøjelsgaard, K., Pichler, D. E., Rasmussen, C., & Woodward, G. (2010). From Broadstone to Zackenberg: Space, time and hierarchies in ecological networks. *Advances in Ecological Research*, *42*, 1–69.

Patefield, W. M. (1981). Algorithm AS159. An efficient method of generating r × c tables with given row and column totals. *Applied Statistics*, *30*, 91–97.

Poisot, T., Canard, E., Mouillot, D., Mouquet, N., & Gravel, D. (2012). The dissimilarity of species interaction networks. *Ecology Letters*, *15*(12), 1353–1361.

Poisot, T., Stouffer, D. B., & Gravel, D. (2015). Beyond species: why ecological interaction networks vary through space and time. *Oikos*, *124*, 243–251.

Polatto, L. P., Chaud-Netto, J., & Alves-Junior, V. V. (2014). Influence of abiotic factors and floral resource availability on daily foraging activity of bees: Influence of abiotic and biotic factors on bees. *Journal of Insect Behavior*, *27*, 593–612.

Ratoni, B., Cruz, C. P., Novais, S., Rodríguez-Morales, D., Neves, F. S., Ayala, R., & Dáttilo, W. (2025). Temporal decay of similarity in bee-plant relationships throughout the day. *Oecologia*, *207*, 2.

Resasco, J., Chacoff, N. P., & Vázquez, D. P. (2021). Plant–pollinator interactions between generalists persist over time and space. *Ecology*, *102*(6), e03359.

Schwarz, B., Vázquez, D. P., CaraDonna, P. J., Knight, T. M., Benadi, G., Dormann, C. F., Gauzens, B., Motivans, E., Resasco, J., Blüthgen, N., Burkle, L. A., Fang, Q., Kaiser-Bunbury, C. N., Alarcón, R., Bain, J. A., Chacoff, N. P., Huang, S. Q., LeBuhn, G., MacLeod, M., … Fründ, J. (2020). Temporal scale-dependence of plant–pollinator networks. *Oikos*, *129*(9), 1289–1302.

Štenc, J., Janošík, L., Matoušková, E., Hadrava, J., Mikát, M., & Janovský, Z. (2023). Pollinator visitation closely tracks diurnal patterns in pollen release. *American Journal of Botany*, *110*(6), e16179.

Stone, G. N., Amos, J. N., Stone, T. F., Knight, R. L., Gay, H., & Parrott, F. (1988). Thermal effects on activity patterns and behavioural switching in a concourse of foragers on *Stachytarpheta mutabilis* (Verbenaceae) in Papua New Guinea. *Oecologia*, *77*, 56–63.

Ulrich, J. K., & Peters, V. E. (2023). Integrating network theory and biodiversity conservation: Do different species selection approaches result in different recommendations? *Biodiversity and Conservation*, *32*(3), 1047–1063.

Vázquez, D. P., Blüthgen, N., Cagnolo, L., & Chacoff, N. P. (2009). Uniting pattern and process in plant–animal mutualistic networks: A review. *Annals of Botany*, *103*(9), 1445–1457.

Vizentin-Bugoni, J., Maruyama, P. K., Debastiani, V. J., Duarte, L. D. S., Dalsgaard, B., & Sazima, M. (2016). Influences of sampling effort on detected patterns and structuring processes of a neotropical plant–hummingbird network. *Journal of Animal Ecology*, *85*(1), 262–272.

Willmer, P. G., & Stone, G. N. (2004). Behavioral, ecological, and physiological determinants of the activity patterns of bees. *Advances in the Study of Behavior*, *34*(34), 347–466.

SUPPORTING INFORMATION

Additional supporting information can be found online in the Supporting Information section at the end of this article.

Figure S1. Sampling completeness profile of the daily sampling periods.

Figure S2. Sampling completeness of the full-day plant–bee interaction network.

Figure S3. Weekly variation in interaction intensity among daily sampling periods.

Figure S4. Intra-seasonal variation in interaction intensity among daily sampling periods.

Figure S5. Pairwise interaction richness across phenological blocks and flowering seasons.

Figure S6. Connectance across phenological blocks and flowering seasons.

Figure S7. Interaction evenness across phenological blocks and flowering seasons.

Figure S8. Network-wide specialisation degree across phenological blocks and flowering seasons.

Figure S9. Weighted nestedness across phenological blocks and flowering seasons.

Figure S10. Weighted modularity across phenological blocks and flowering seasons.

Figure S11. Intra-seasonal phenological variation interaction β-diversity among daily sampling periods.

Figure S12. Plant–bee interaction β-diversity among each partial- and the full-day network and across phenological blocks and flowering seasons.

Table S1. List of bee taxa recorded in the study and their interaction patterns.

Table S2. Mixed-model specifications used to test temporal variation in network structure and pairwise interaction turnover across sampling periods.

Table S3. Full model selection table (AICc) for testing whether intra-seasonal blocks (early-, mid- and late-season) modify daily patterns of interaction β-diversity (β^{WN}).

Table S4. Hierarchical variance partitioning of interaction β-diversity (β^{WN}) across intraday and seasonal temporal scales.

How to cite this article: Ballarin, C. S., Isla, J., Arroyo-Correa, B., Quintero, E., Hachuy-Filho, L., Amorim, F. W., & Jordano, P. (2026). Optimising daily sampling of plant–bee interaction networks. *Journal of Animal Ecology*, *00*, 1–16. https://doi.org/10.1111/1365-2656.70309

Supplementary material

Optimising daily sampling of plant–bee interaction networks

Caio S. Ballarin[1,2,3*], Jorge Isla[3], Blanca Arroyo-Correa[3], Elena Quintero[3,4], Leandro Hachuy-Filho[1,5], Felipe W. Amorim[1,2,5a], Pedro Jordano[3,4a]

[1] Laboratório de Ecologia da Polinização e Interações – LEPI, Departamento de Biodiversidade e Bioestatística, Instituto de Biociências, Universidade Estadual Paulista "Júlio de Mesquita Filho" (UNESP), Rua Prof. Dr. Antonio Celso Wagner Zanin, CEP 18618-689, Botucatu, São Paulo State, Brazil

[2] Programa de Pós-graduação em Biologia Vegetal, Instituto de Biociências, Universidade Estadual Paulista "Júlio de Mesquita Filho"

[3] Integrative Ecology Group, Estación Biológica de Doñana, EBD-CSIC, Av. Américo Vespucio 26, E-41092 Sevilla, Spain

[4] Departamento de Biología Vegetal y Ecología, Universidad de Sevilla, Av. Reina Mercedes, E-41012 Sevilla, Spain

[5] Programa de Pós-graduação em Zoologia, Instituto de Biociências, Universidade Estadual Paulista "Júlio de Mesquita Filho"

[a] co-senior authors

Correspondence: Caio S. Ballarin

E-mail address: csballarin@gmail.com

Content

Supplementary Methods — Seasonal analyses

Seasonal consistence of daily interaction patterns

Interaction frequency and richness

Because flowering and pollinator phenology vary markedly across the season in the Cerrado (Ballarin et al. 2026), we conducted additional analyses to evaluate whether intra- and inter-seasonal variation could bias comparisons among daily sampling periods.

First, we visually explored the logarithm of (i) interaction frequency and (ii) pairwise interaction richness for each daily sampling period across all sampling weeks in both flowering seasons (Figure S3). This exploratory analysis aimed to assess whether the relative contribution of each daily period to total interaction activity and interaction richness changed across weeks or between seasons, which would indicate a potential seasonal permutation in the dominance of daily periods.

Second, because sampling was conducted weekly over 30 weeks in each flowering season, we divided the sampling period into three phenological blocks: early-, mid-, and late-season, which broadly reflect seasonal changes in solar radiation, temperature, and humidity. We then visually explored interaction frequency and pairwise interaction richness among daily periods within each of these three seasonal blocks to assess whether daily patterns were consistent across the season (Figure S4).

Network structure

Third, we quantified network structure across sampling periods by constructing interaction networks for each combination of flowering season, phenological block (early-, mid-, and late-season), plot, and 2-h sampling interval. From these networks, we calculated pairwise interaction richness, connectance (C), interaction evenness (IE), network-level specialisation (H2’), weighted nestedness (wNODF), and weighted modularity (Qw’). For nestedness and modularity, we used Δ-transformed values (ΔwNODF and ΔQw’) based on null model expectations.

Detailed descriptions of these metrics are provided in the main text (Materials and Methods).

We then visually inspected the distribution of these network metrics across sampling periods, flowering seasons, and phenological blocks (early-, mid-, and late-season) to assess how network structure varies within the day and if this pattern is consistent within and across flowering seasons (Figure S5 – S10).

Interaction β-diversity

Fourth, to formally test whether seasonal variation in species occurrence could influence interaction turnover and bias our β-diversity results, we repeated the interaction network analyses separately for each phenological block. For each block, we built interaction networks for each plot, flowering season, and daily sampling period by aggregating all interactions recorded within that block. Within each block, and following exactly the same approach described in the main text, we calculated overall interaction β-diversity (β^{WN}) among daily sampling periods (Figure S11a).

We then fitted generalized linear mixed models with beta error distribution, using β^{WN} as the response variable and including the interaction between daily period comparison (e.g., 06:00-08:00h *versus* 08:00-10:00h), and phenological block (i.e., early-, mid-, late-season), as well as flowering season (i.e., first and second flowering season), as fixed effects, and plot identity as a random effect. Model selection was performed using the dredge function in the *MuMIn* package, and models were ranked using AICc (Table S3). If intra-seasonal phenological variation strongly influenced the daily patterns reported in the main text, the best-supported models would be expected to include interactions between daily period and phenological block.

In addition, to quantify the relative contribution of intraday *versus* seasonal processes to interaction β-diversity, we adopted a hierarchical variance decomposition approach based on a sequence of generalized linear mixed models with beta error distribution. We first fitted a null model including only plot identity as a random effect. We then added daily period comparison as a fixed effect to test how much variance is explained solely by intraday temporal structure. Next, we added phenological block (early-, mid-, late-season) to account for intra-seasonal variation in species composition. Finally, we fitted the full model including

flowering season and all interactions among factors. For each model, we computed marginal R^2 (Nakagawa & Schielzeth, 2013) and quantified the incremental increase in explained variance (ΔR^2) between successive models (Table S4). This approach allows disentangling the variance attributable to intraday temporal organization from that associated with seasonal phenological turnover.

Finally, for each phenological block (early, mid, late), we calculated Spearman correlations between temporal distance among daily periods and interaction β-diversity (β^{WN}) (Figure S11b-d). Similar magnitude and direction of these correlations across blocks would indicate that the variation in interaction dissimilarity across daily sampling periods is consistent even when controlling for intra-seasonal phenological variation.

Representativeness of partial-day networks in resembling the full day network

Fifth, to assess how well different sampling periods capture daily interaction patterns, we compared partial-day networks (i.e., networks constructed from single or combined 2-h intervals) with a full-day reference network. For each flowering season and phenological block, the full-day network was built by pooling all sampling periods and used as a benchmark.

We generated all possible combinations of sampling periods and constructed the corresponding partial-day networks. Representativeness was evaluated by measuring interaction β-diversity (β^{WN}) between each partial-day network and the corresponding full-day network, as described in the main text (Materials and Methods).

Lower β-diversity values indicate that a given sampling combination more closely approximates the full set of daily interactions. We visually inspected these patterns to identify which sampling periods or combinations best represent daily interaction structure across flowering seasons and phenological blocks (Figure S12).

All graphical and statistical results of these analyses are presented in Figures S3–S12 and Table S3 and S4.

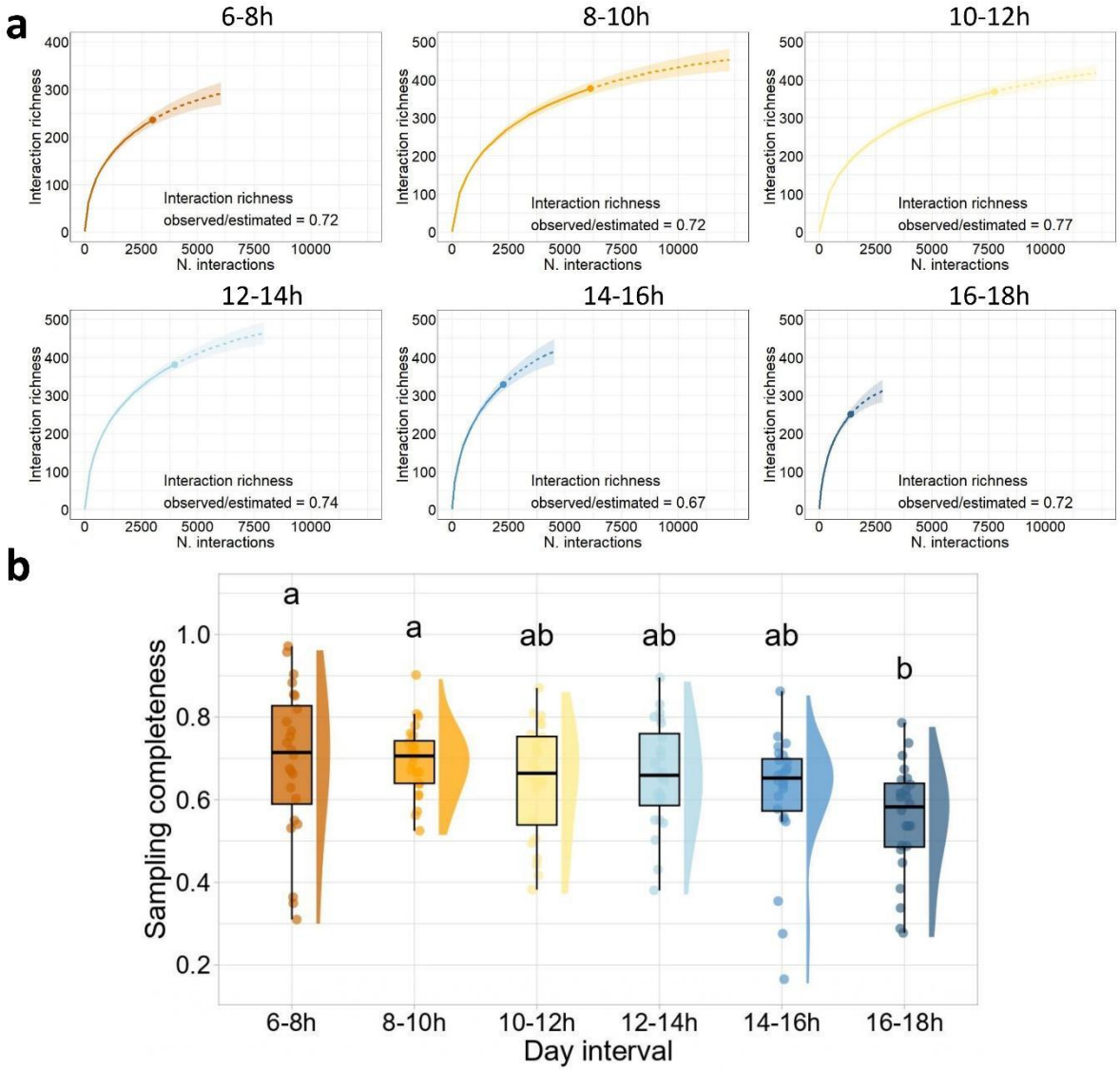

Figure S1. Sampling completeness profile of the daily sampling periods. The completeness of plant–bee pairwise interaction inventories for each sampling period, pooling interaction data from all plots (a). Empirical plant–bee interaction richness reached a modal value of 72.33 ± 3.27% compared to what could be expected if all pairwise interactions were sampled. Comparisons of sampling completeness among 2-hour sampling periods within each plot (b) revealed slight differences, with late afternoon (i.e., 16-18h) showing the lowest score.

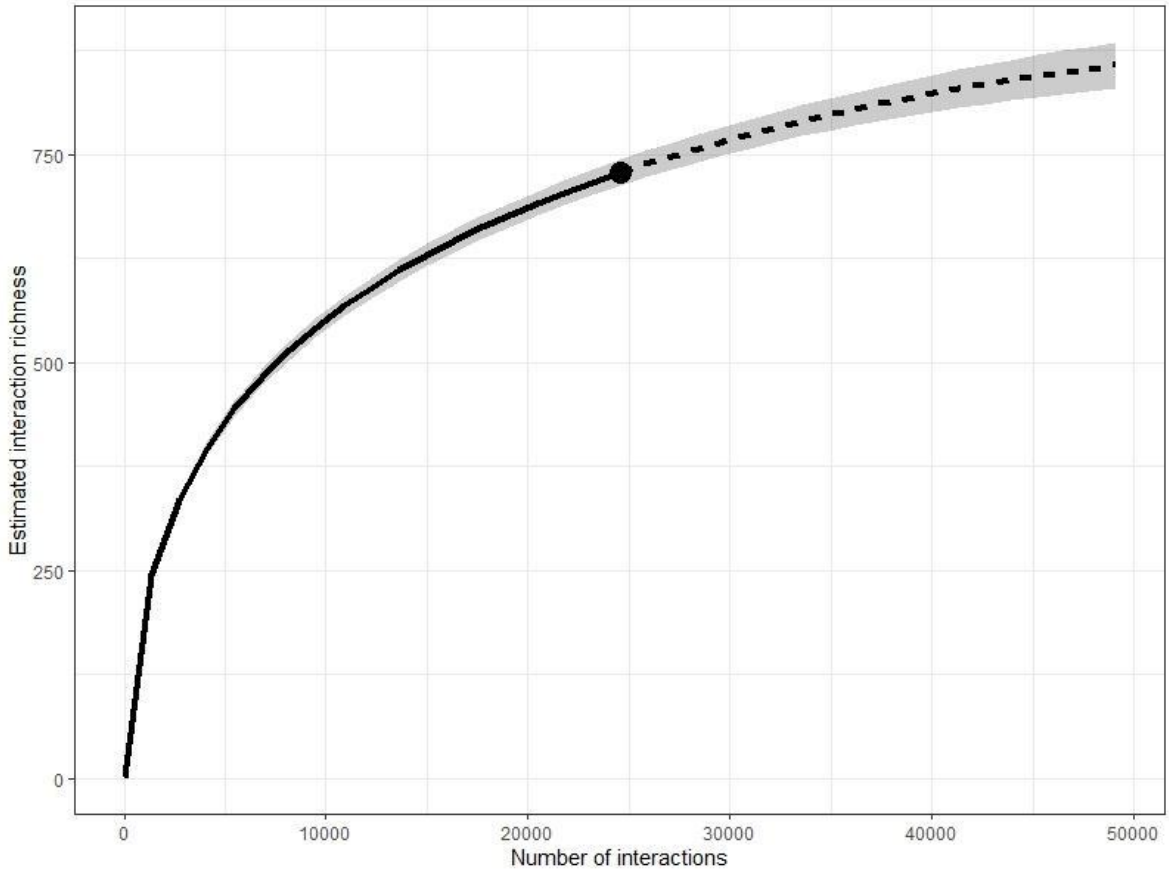

Figure S2. Sampling completeness of the full-day plant–bee interaction network. Rarefaction and extrapolation curve of interaction richness for the full-day network, built by combining all sampling periods and plots. The solid line represents the rarefaction curve based on the observed data, and the dashed line represents the extrapolation beyond the observed sampling effort. The shaded area indicates 95% confidence intervals. The black dot marks the observed sampling effort. Sampling completeness was quantified as the ratio between the number of observed interactions and the estimated total interaction richness, indicating that approximately 78% of the estimated plant–bee pairwise interactions were captured by the full-day network.

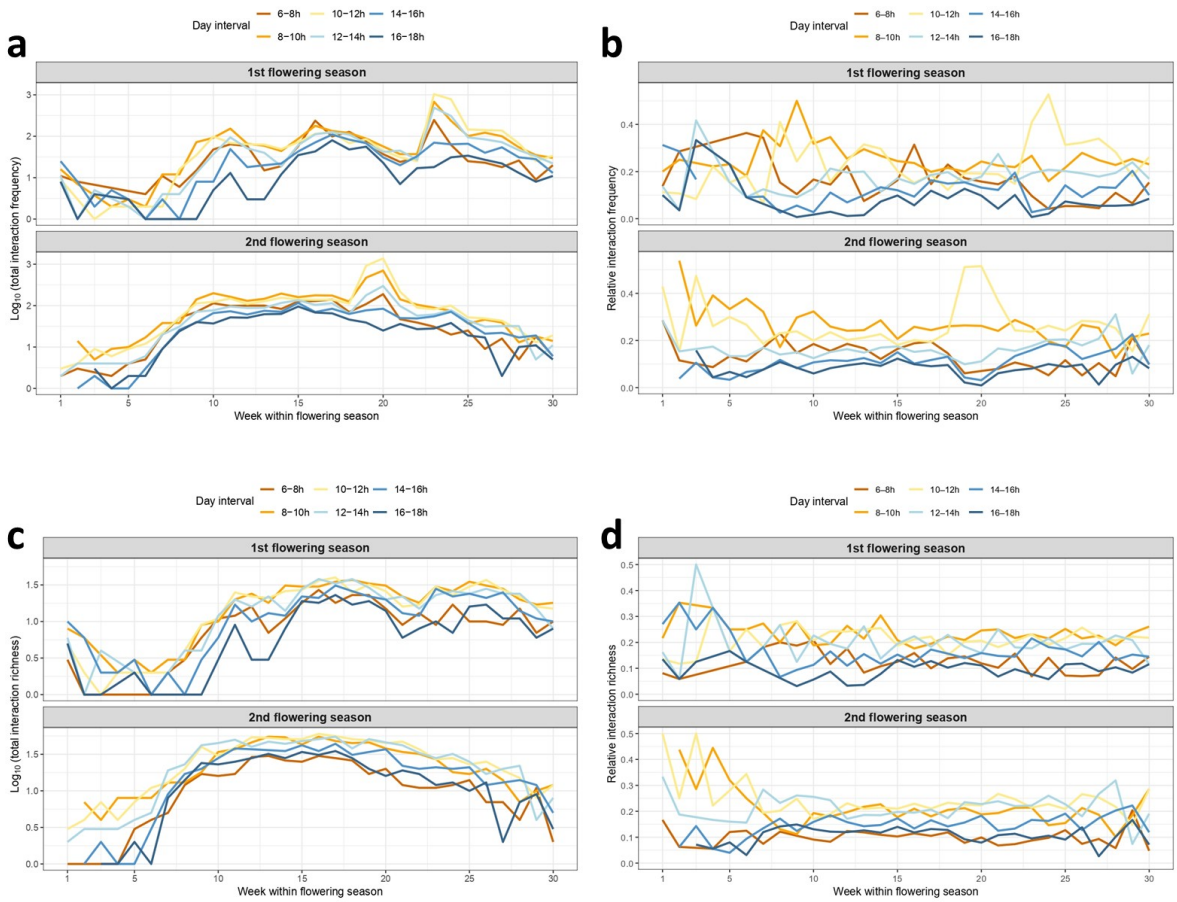

Figure S3. Weekly variation in interaction intensity among daily sampling periods. Panels (a) and (c) show the temporal dynamics of $\log_{10}$-transformed total interaction frequency and $\log_{10}$-transformed total interaction richness, respectively, across the weeks of sampling within the first and second flowering seasons. Panels (b) and (d) show the corresponding relative interaction frequency and relative interaction richness, expressed as the proportion of all interactions recorded in each week that occurred in each 2h -daily period (e.g., 6-8h, 8-10h). Although both interaction frequency and richness exhibit marked intraseasonal variation, reflecting changes in plant and pollinator occurrence associated with their phenologies, the relative ranking among daily periods remains largely consistent through time: periods with higher interaction frequency and richness tend to remain higher across weeks, whereas periods with lower values remain consistently lower. This indicates that, despite strong intraseasonal fluctuations in the overall availability of interactions, the structure of interaction allocation among daily periods is relatively stable. Together, these results show that intraseasonal phenological variation affects the magnitude of interactions but does not substantially modify the comparative differences among daily sampling periods.

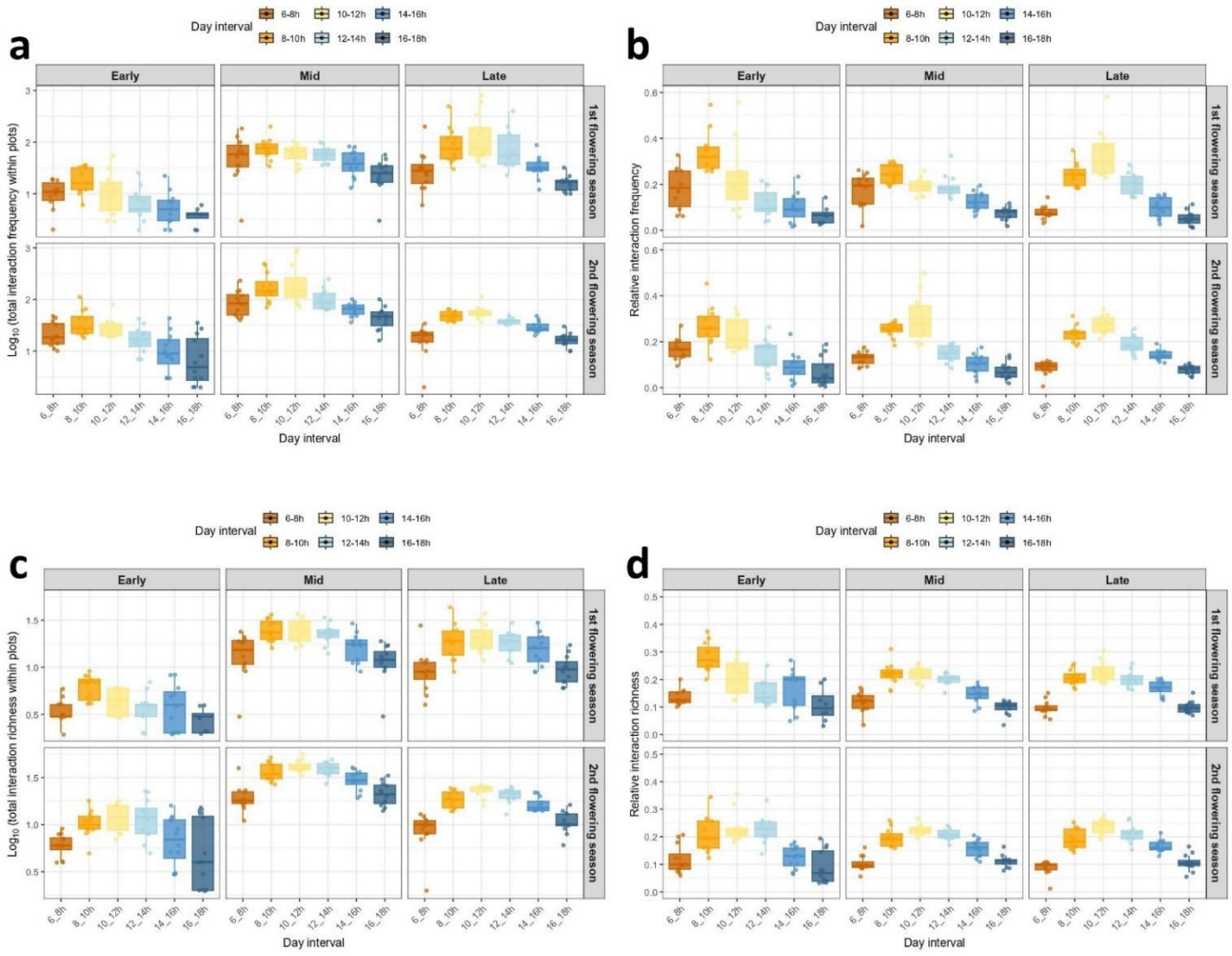

Figure S4. Intraseasonal variation in interaction intensity among daily sampling periods. Panels (a) and (c) show $\log_{10}$-transformed total interaction frequency and $\log_{10}$-transformed total interaction richness, respectively, summarized for each phenological block (early, mid, and late-season) in the first and second flowering seasons. Panels (b) and (d) show the corresponding relative interaction frequency and relative interaction richness, expressed as the proportion of all interactions recorded within each phenological block that occurred in each daily period. In contrast to the week-by-week representation, this block-level aggregation further emphasizes that daily periods consistently differ in their interaction intensity, with periods showing higher frequency and richness remaining higher across phenological blocks, and periods with lower values remaining consistently lower. This indicates that, even when accounting for intraseasonal shifts in plant and pollinator occurrence associated with phenology, the allocation of interactions among daily periods is highly stable across the flowering season. Thus, phenological turnover modifies the overall magnitude of interactions but does not alter the relative differences among daily sampling periods.

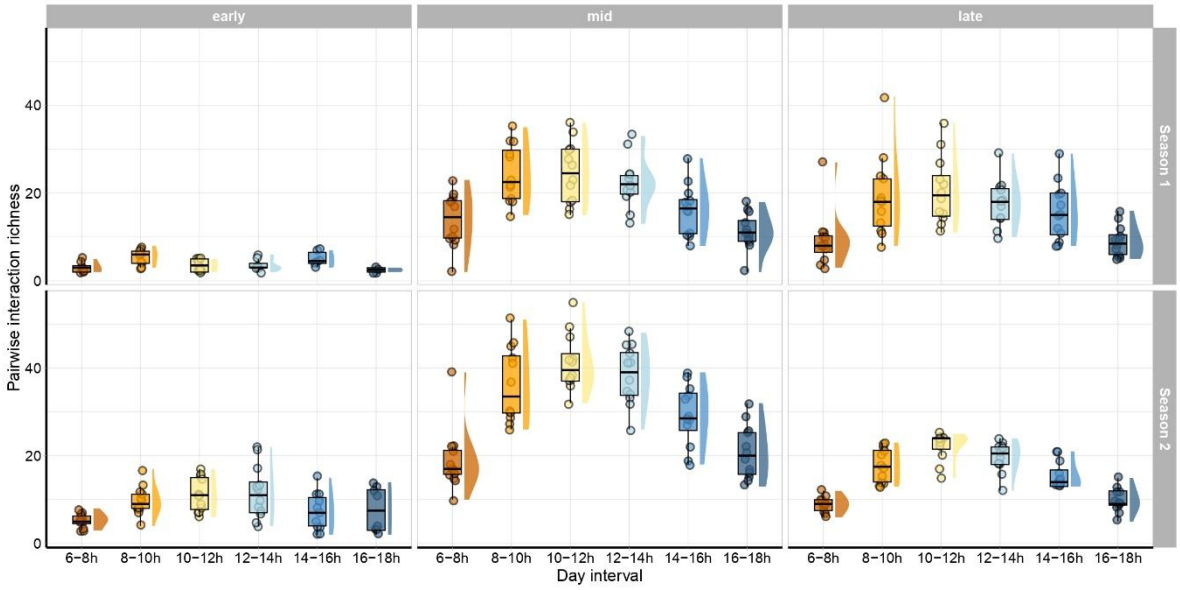

Figure S5. Pairwise interaction richness across phenological blocks and flowering seasons. Boxplots with accompanying violin plots depict the distribution of pairwise interaction richness across 2-h sampling intervals (6–8h, 8–10h, 10–12h, 12–14h, 14–16h, 16–18h), color-coded along the orange–blue continuum to represent progression from early morning to late afternoon. Data are partitioned by flowering season (Season 1: 2021/2022; Season 2: 2022/2023) and subdivided into early, mid, and late phenological blocks (10 weeks each). While seasonal structuring introduces some variation, the dominant signal remains the within-day dynamics: pairwise interaction richness is consistently higher near midday, revealing a temporal pattern that parallels the intra-day trends described in Figure 1a.

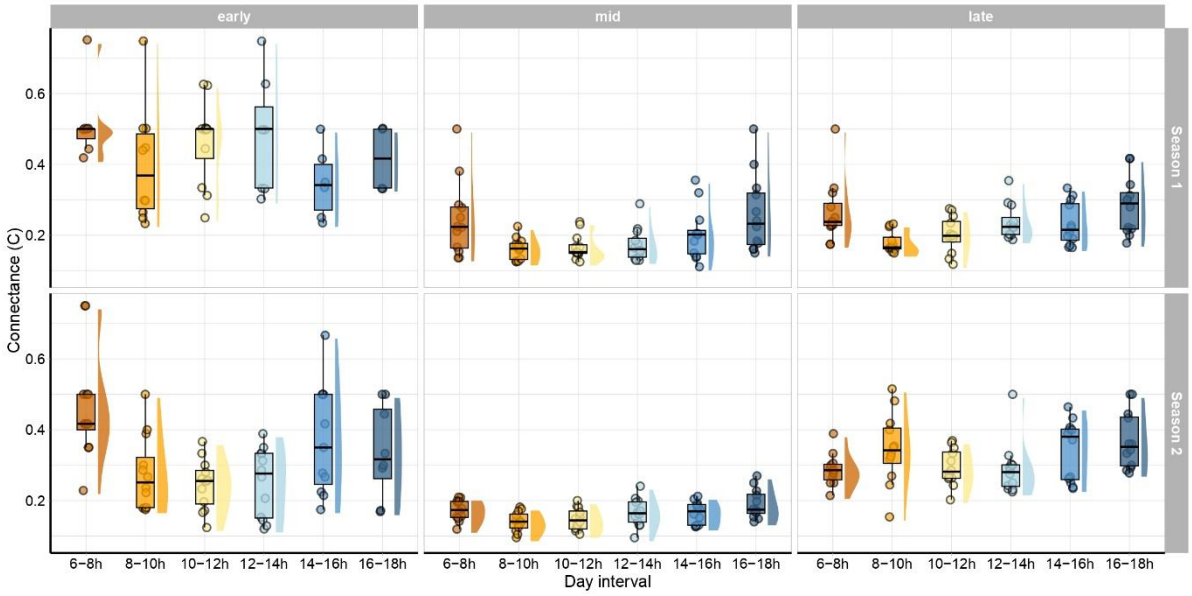

Figure S6. Connectance across phenological blocks and flowering seasons. Boxplots with accompanying violin plots depict the distribution of connectance (C) across 2-h sampling intervals (6–8h, 8–10h, 10–12h, 12–14h, 14–16h, 16–18h), color-coded along the orange–blue continuum to represent progression from early morning to late afternoon. Data are partitioned by flowering season (Season 1: 2021/2022; Season 2: 2022/2023) and subdivided into early, mid, and late phenological blocks (10 weeks each). Although seasonal structuring introduces some deviations, particularly during the early-season, the dominant signal remains the within-day variation: C values tend to peak at both dawn and dusk, revealing a temporal pattern broadly aligned with that described in Figure 1b.

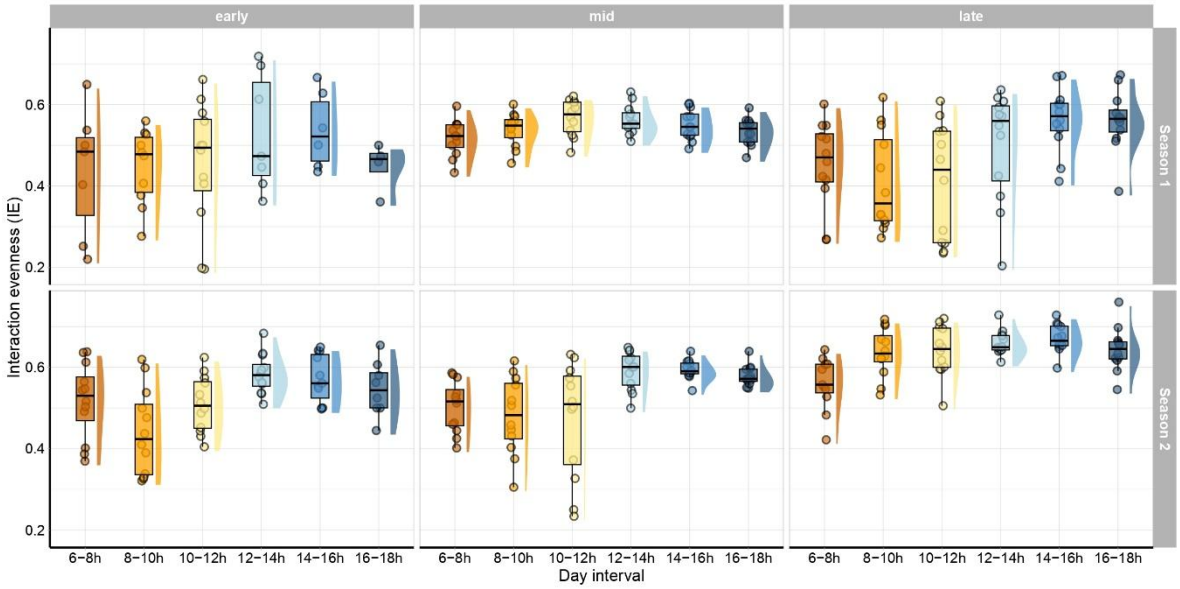

Figure S7. Interaction evenness across phenological blocks and flowering seasons. Boxplots with accompanying violin plots depict the distribution of interaction evenness (IE) across 2-h sampling intervals (6–8h, 8–10h, 10–12h, 12–14h, 14–16h, 16–18h), color-coded along the orange–blue continuum to represent progression from early morning to late afternoon. Data are partitioned by flowering season (Season 1: 2021/2022; Season 2: 2022/2023) and subdivided into early, mid, and late phenological blocks (10 weeks each). Although seasonal structuring introduces some deviations, particularly during the early-season, the dominant signal remains the within-day variation: IE increases progressively throughout the day, reaching higher values during sampling periods after midday, revealing a temporal pattern that parallels the intra-day trends described in Figure 1c.

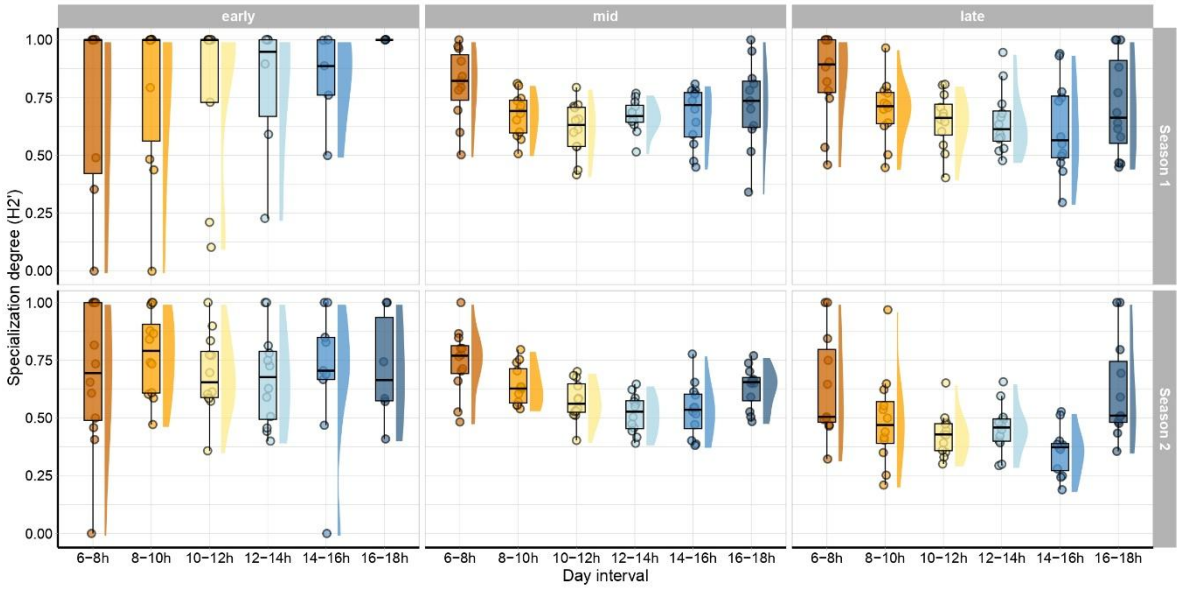

Figure S8. Network-wide specialization degree across phenological blocks and flowering seasons. Boxplots with accompanying violin plots depict the distribution of specialization degree (H2′) across 2-h sampling intervals (6–8h, 8–10h, 10–12h, 12–14h, 14–16h, 16–18h), color-coded along the orange–blue continuum to represent progression from early morning to late afternoon. Data are partitioned by flowering season (Season 1: 2021/2022; Season 2: 2022/2023) and subdivided into early, mid, and late phenological blocks (10 weeks each). Although seasonal structuring introduces some deviations, particularly during the early-season, the dominant signal remains the within-day variation: H2' is highest in the early morning (6–8h), with a relative increase again toward dusk, revealing a temporal pattern broadly aligned with that described in Figure 1d.

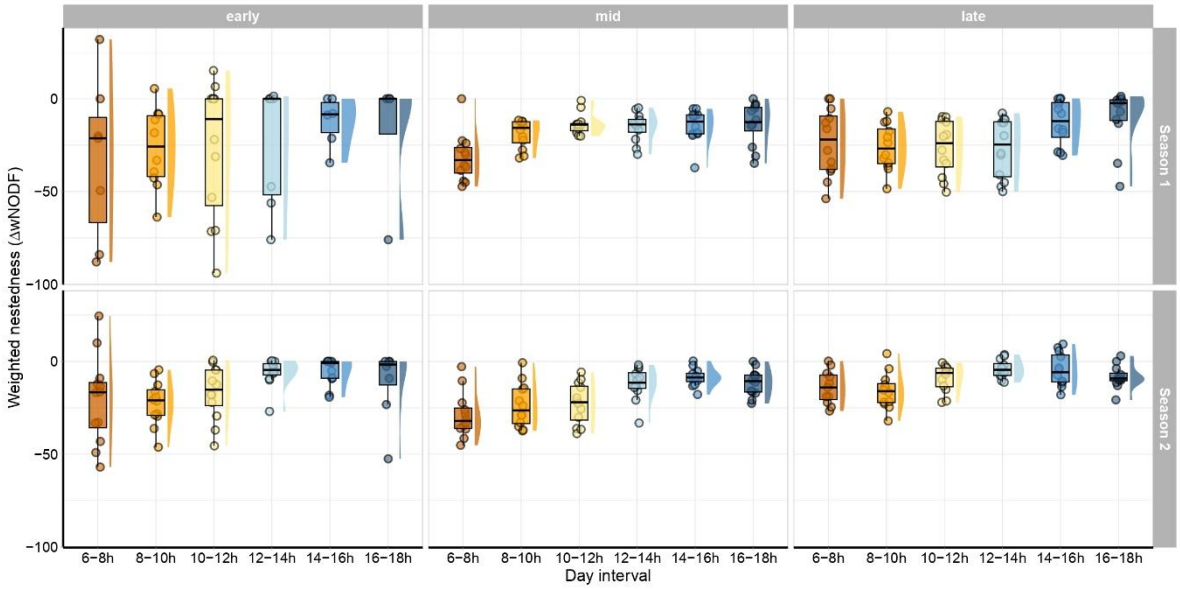

Figure S9. Weighted nestedness across phenological blocks and flowering seasons. Boxplots with accompanying violin plots depict the distribution of weighted nestedness (ΔwNODF) across 2-h sampling intervals (6–8h, 8–10h, 10–12h, 12–14h, 14–16h, 16–18h), color-coded along the orange–blue continuum to represent progression from early morning to late afternoon. Data are partitioned by flowering season (Season 1: 2021/2022; Season 2: 2022/2023) and subdivided into early, mid, and late phenological blocks (10 weeks each). Although seasonal structuring introduces some deviations, particularly during the early-season, the dominant signal remains the within-day variation: ΔwNODF increases progressively throughout the day, reaching higher values during sampling periods after midday. This reveals a temporal pattern that parallels the intra-day trends described in Figure 1e.

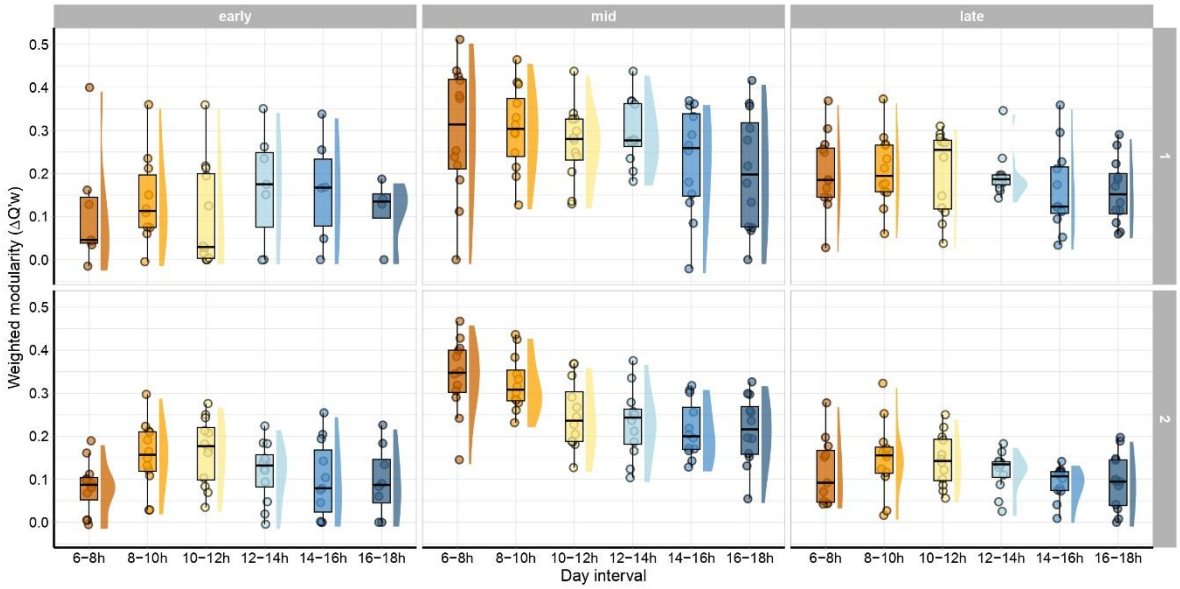

Figure S10. Weighted modularity across phenological blocks and flowering seasons. Boxplots with accompanying violin plots depict the distribution of weighted nestedness (ΔQw') across 2-h sampling intervals (6–8h, 8–10h, 10–12h, 12–14h, 14–16h, 16–18h), color-coded along the orange–blue continuum to represent progression from early morning to late afternoon. Data are partitioned by flowering season (Season 1: 2021/2022; Season 2: 2022/2023) and subdivided into early, mid, and late phenological blocks (10 weeks each). Although seasonal structuring introduces some deviations, particularly during the early-season, the dominant signal remains the within-day variation: ΔQw' decreasing progressively throughout the day, reaching lower values toward dusk. This reveals a temporal pattern that parallels the intra-day trends described in Figure 1f.

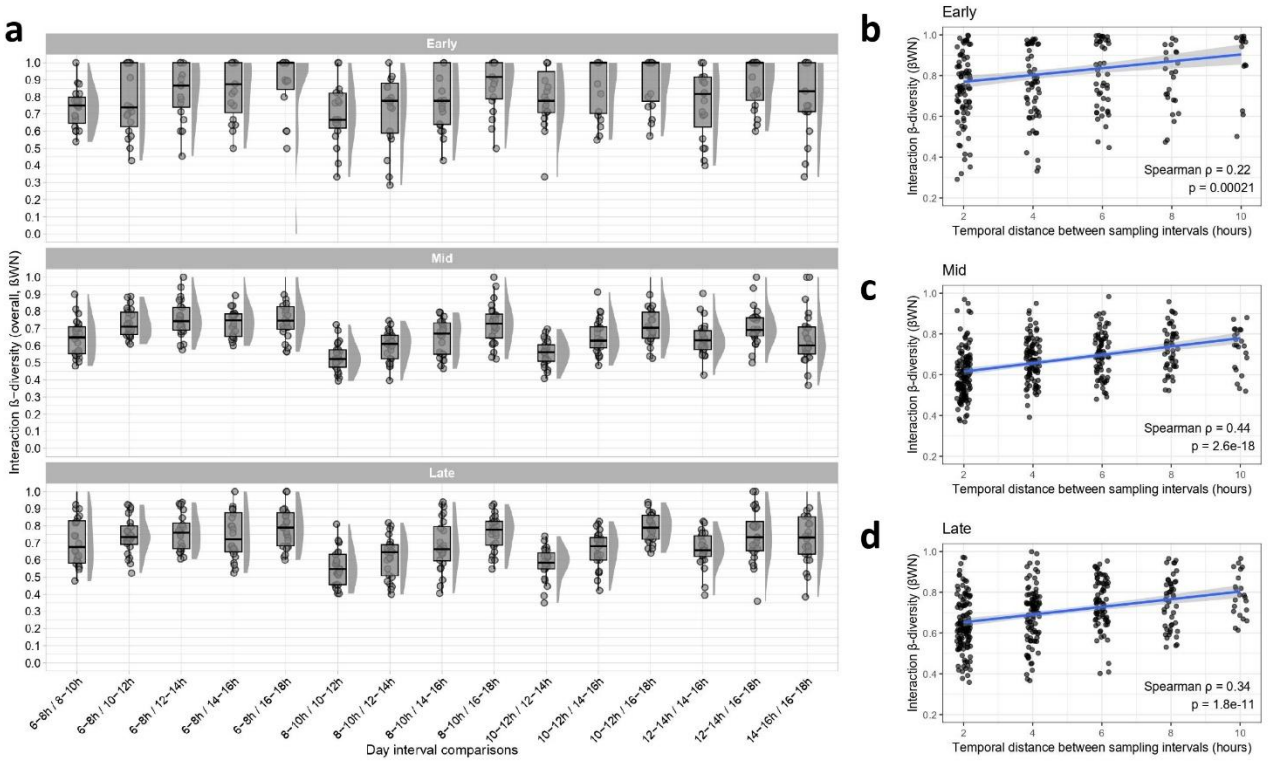

Figure S11. Intra-seasonal phenological variation interaction β-diversity among daily sampling periods. Panel (a) shows the distribution of interaction β-diversity (β^{WN}) among all pairwise daily period comparisons, calculated separately for each phenological block (early-, mid-, late-season) after aggregating all interactions within each block for each plot and flowering season. Across blocks, β^{WN} values exhibit highly similar distributions, indicating that interaction β-diversity among daily periods follows comparable patterns at the beginning, middle, and end of the flowering season. Panels (b–d) show, for each phenological block (early-, mid-, late-season, respectively), the relationship between temporal distance between sampling periods (in hours) and interaction β-diversity (β^{WN}). In all three blocks, interaction dissimilarity increases with increasing temporal distance, as indicated by the positive and significant Spearman correlations. Together, these results demonstrate that although species composition changes within the flowering season due to phenology, the temporal scaling of interaction β-diversity among daily periods remains consistent, and the higher β-diversity observed between more distant daily periods is independent of whether comparisons are made early, mid, or late in the flowering season.

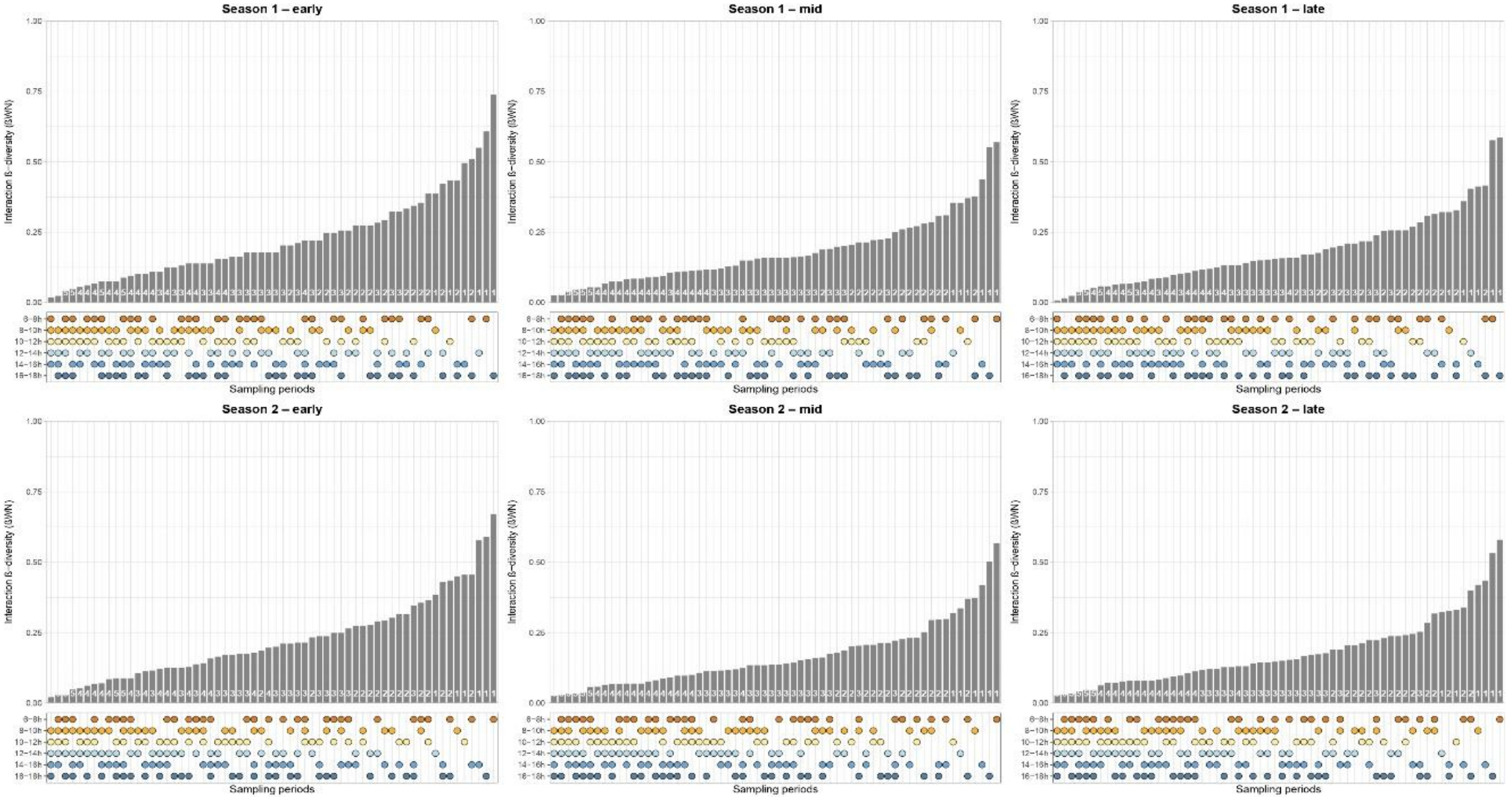

Figure S12. Plant–bee interaction β-diversity among each partial- and the full-day network and across phenological blocks and flowering seasons. The bar plots represent the overall β-diversity of plant–bee interactions (i.e., βWN) among partial-day networks

across phenological blocks (early, mid, late; each spanning 10 weeks) and flowering seasons (Season 1 and Season 2). Each bar corresponds to a partial-day network, indicating which sampling periods were combined to create the interaction matrix. Circles below the graphs are colored following the orange–blue continuum (from 6-8h – dark orange – to 16–18h – dark blue) and ordered according to the number of sampling periods that were merged to build the network. The numbers within each bar denote the number of sampling periods that were merged. Patterns across phenological blocks and flowering seasons follow the same trend described in Figure 4: interaction composition dissimilarities (βWN) between full- and partial-day networks generally decreased as additional 2-h sampling periods were included. Although some variation is evident, particularly in the early-season blocks, the representativeness of partial-day networks remains similar, with central 2-h periods (from 8-10h to 12-14h) being the most informative and consistently reducing β-diversity more strongly than other combinations.

Table S1. List of bee taxa recorded in the study and their interaction patterns. For each bee taxon, the table reports the type of floral resource collected (e.g., nectar, pollen, oil, resin), the main foraging behaviour (e.g., generalist, specialist, buzz-pollination, oil-collecting), the absolute frequency of interactions, and the relative frequency of interactions (expressed as the proportion of all recorded interactions in the dataset). In addition, the table details the distribution of interactions across the six 2-h daily sampling intervals, allowing the visualization of temporal variation in foraging activity throughout the day.

Bee species	Interaction frequency	% frequency	Foraging behaviour	Resource collected	Interaction timing					
					6-8h	8-10h	10-12h	12-14h	14-16h	16-18h
Acanthopus excellens	6	0.02	-	Nectar/Pollen	0	3	0	3	0	0
Agapostemum sp1	3	0.01	Buzz	Nectar/Pollen	0	0	1	1	1	0
Ancyloscelis apiformis	21	0.09	-	Nectar/Pollen	1	8	6	5	1	0
Anthidiini sp1	15	0.06	-	Nectar/Pollen	0	4	3	5	2	1
Apis mellifera	11858	48.31	-	Nectar/Pollen	1343	3389	4881	1450	546	249
Augochlora sp1	21	0.09	Buzz	Nectar/Pollen	0	6	2	5	5	3
Augochloropsis sp1	207	0.84	Buzz	Nectar/Pollen	14	46	51	35	41	20
Augochloropsis sp2	5	0.02	Buzz	Nectar/Pollen	0	1	0	1	2	1
Augochloropsis sp3	116	0.47	Buzz	Nectar/Pollen	4	24	41	18	19	10
Bombus morio	731	2.98	Buzz	Nectar/Pollen	111	179	113	130	109	89
Bombus pauloensis	52	0.21	Buzz	Nectar/Pollen	9	13	3	5	7	15
Centris sp1	9	0.04	Oil/Buzz	Nectar/Pollen/Oil	1	1	0	2	3	2
Centris sp2	154	0.63	Oil/Buzz	Nectar/Pollen/Oil	0	11	35	61	44	3
Centris sp3	584	2.38	Oil/Buzz	Nectar/Pollen/Oil	102	144	115	96	83	44
Centris sp4	23	0.09	Oil/Buzz	Nectar/Pollen/Oil	0	22	1	0	0	0
Centris sp5	71	0.29	Oil/Buzz	Nectar/Pollen/Oil	6	4	6	11	26	18
Centris sp6	29	0.12	Oil/Buzz	Nectar/Pollen/Oil	19	10	0	0	0	0
Centris sp7	24	0.10	Oil/Buzz	Nectar/Pollen/Oil	5	7	2	1	5	4
Centris sp8	63	0.26	Oil/Buzz	Nectar/Pollen/Oil	19	18	5	10	7	4
Ceratalictus sp1	115	0.47	Buzz	Nectar/Pollen	9	29	27	19	17	14

Ceratina sp1	4	0.02	-	Nectar/Pollen	0	0	2	1	0	1
Ceratina sp2	1611	6.56	-	Nectar/Pollen	85	379	441	358	228	120
Dialictus sp1	1	0.00	-	Nectar/Pollen	0	0	0	1	0	0
Emphorini sp2	22	0.09	-	Nectar/Pollen	0	13	4	2	2	1
Emphorini sp3	62	0.25	-	Nectar/Pollen	9	25	16	8	4	0
Emphorini sp4	82	0.33	-	Nectar/Pollen	3	13	18	25	18	5
Epicharis sp1	333	1.36	Oil/Buzz	Nectar/Pollen/Oil	142	51	17	23	33	67
Epicharis sp2	145	0.59	Oil/Buzz	Nectar/Pollen/Oil	45	29	17	9	18	27
Epicharis sp3	255	1.04	Oil/Buzz	Nectar/Pollen/Oil	118	65	27	17	15	13
Epicharis sp4	16	0.07	Oil/Buzz	Nectar/Pollen/Oil	0	7	2	1	2	4
Eucerini sp2	5	0.02	-	Nectar/Pollen	0	1	2	2	0	0
Eufriesea sp1	16	0.07	Buzz	Nectar/Pollen/Fragrance	4	8	1	0	0	3
Euglossa sp1	8	0.03	Buzz	Nectar/Pollen/Fragrance	0	1	4	2	0	1
Eulaema nigrita	169	0.69	Buzz	Nectar/Pollen/Fragrance	51	51	28	9	8	22
Exomalopsis analis	5	0.02	Buzz	Nectar/Pollen	1	0	3	0	1	0
Exomalopsis fulvofasciata	50	0.20	Buzz	Nectar/Pollen	3	12	7	9	11	8
Frieseomelitta varia	13	0.05	-	Nectar/Pollen/Resin	0	8	3	1	0	1
Mesoplia sp1	112	0.46	-	Nectar/Pollen	2	4	27	23	26	30
Nannotrigona sp1	20	0.08	-	Nectar/Pollen	0	4	0	13	1	2
Oxaea flavescens	43	0.18	Buzz	Nectar/Pollen	19	5	9	6	2	2
Paratrigona sp1	2464	10.04	-	Nectar/Pollen	137	580	677	592	340	138
Paroxystoglossa sp1	12	0.05	Buzz	Nectar/Pollen	0	2	5	0	4	1
Plebeia sp1	32	0.13	-	Nectar/Pollen	7	11	3	2	7	2
Ptiloglossa sp1	71	0.29	Buzz	Nectar/Pollen	71	0	0	0	0	0
Tapinotaspidini sp1	26	0.11	Oil	Nectar/Pollen/Oil	0	3	4	14	5	0
Tapinotaspidini sp2	116	0.47	Oil	Nectar/Pollen/Oil	24	23	35	18	10	6
Tapinotaspidini sp3	247	1.01	Oil	Nectar/Pollen/Oil	14	65	94	57	14	3
Temnosoma sp1	27	0.11	-	Nectar/Pollen	2	8	5	5	6	1
Tetragonisca angustula	648	2.64	-	Nectar/Pollen/Resin	8	56	263	278	42	1

Trigona spinipes	2725	11.10	-	Nectar/Pollen/Resin	173	425	668	541	508	410
Xylocopa sp1	70	0.29	Buzz	Nectar/Pollen	31	32	1	0	4	2
Xylocopa sp2	1029	4.19	Buzz	Nectar/Pollen	419	330	87	96	41	56

Table S2. Mixed-model specifications used to test temporal variation in network structure and pairwise interaction turnover across sampling periods. Response variables, predictor variables, random-effect structure, and error distributions used in the generalized linear mixed models (GLMMs) and linear mixed models (LMMs). Network structure metrics (pairwise interaction richness, connectance *C*, interaction evenness *IE*, specialization *H2'*, weighted nestedness *wNODF*, and weighted modularity *Qw'*) were modeled as a function of the 2-h sampling period, with season and plot identity included as crossed random effects. Pairwise interaction turnover (β^{WN}) was modeled as a function of the comparison between sampling periods, using the same random-effect structure. Beta-regression models were fitted using a logit link, Poisson models used a log link, and Gaussian models used an identity link.

Response variable	Predictor	Random effects	Error distribution	Link function
Pairwise interaction richness	Sampling period (2-h)	Season + Plot	Poisson	Log
C (connectance)	Sampling period (2-h)	Season + Plot	Beta	Logit
IE (interaction evenness)	Sampling period (2-h)	Season + Plot	Beta	Logit
H2' (specialization degree)	Sampling period (2-h)	Season + Plot	Beta	Logit
wNODF (weighted nestedness)	Sampling period (2-h)	Season + Plot	Gaussian	Identity
Qw' (weighted modularity)	Sampling period (2-h)	Season + Plot	Beta	Logit
β^{WN}	Comparison between sampling periods	Season + Plot	Beta	Logit

Table S3. **Full model selection table (AICc) for testing whether intraseasonal blocks (early-, mid-, and late-season) modify daily patterns of interaction β-diversity (β^{WN}).** Models are generalized linear mixed models with beta error distribution, including plot identity as a random effect in all models. Fixed effects include daily period comparisons (DC), phenological structure (PS), flowering season (Season), and their interactions. Models were ranked by AICc using the dredge function in the 'MuMIn' package. In the table, "+" indicates that the variable or interaction term is included in the model, whereas "–" indicates that it is not included. The Akaike weight (Weight in the Table) represents the relative probability that a given model is the best-supported model among the candidate set, given the data and the set of models considered. Only two models received any substantial support ($\Delta AICc \leq 4$; above the dashed line), and none of them includes the interaction between daily period comparisons and phenological block, indicating that intra-seasonal phenological variation does not modify the daily pattern of interaction β-diversity.

Model	DC	PS	Season	DC×PS	DC×Season	PS×Season	DC×PS×Season	df	logLik	ΔAICc	Weight
40	+	+	+	–	+	–	–	22	729.953	0.00	0.88
8	+	+	+	–	–	–	–	20	725.871	3.99	0.12
56	+	+	+	+	–	+	–	50	751.758	16.71	0.00
24	+	+	+	+	–	–	–	48	747.586	20.63	0.00
48	+	+	+	–	+	–	–	36	733.494	22.64	0.00
16	+	+	+	–	–	–	–	34	729.398	26.53	0.00
64	+	+	+	+	–	+	–	64	755.637	40.45	0.00
32	+	+	+	+	–	–	–	62	751.481	44.21	0.00
6	+	+	–	–	–	–	–	19	695.774	62.10	0.00
128	+	+	+	+	–	+	+	92	776.165	65.31	0.00
22	+	+	–	+	–	–	–	47	717.252	79.09	0.00
39	–	+	+	–	–	–	–	8	649.753	131.51	0.00
7	–	+	+	–	–	–	–	6	647.436	132.09	0.00
5	–	–	+	–	–	–	–	5	622.078	180.78	0.00
4	+	+	–	–	–	–	–	18	506.200	439.17	0.00
2	+	–	–	–	–	–	–	17	496.045	457.41	0.00
12	+	+	–	–	–	+	–	32	511.286	458.48	0.00
3	–	+	–	–	–	–	–	4	445.701	531.51	0.00
1	–	–	–	–	–	–	–	3	437.163	546.57	0.00

Table S4. Hierarchical variance partitioning of interaction β-diversity (β^{WN}) across intraday and seasonal temporal scales. We fitted sequential generalized linear mixed models with beta error distribution, including plot identity as a random effect. Marginal R^2 indicates the variance explained by fixed effects, while conditional R^2 includes both fixed and random effects. ΔR^2 represents the incremental increase in explained variance after adding biologically meaningful blocks of predictors and interaction terms: intraday temporal structure, seasonal phenological structure (i.e., early-, mid-, and late-season), and flowering season (i.e., first and second flowering season; full model). Random effects alone (M0) explained 0% of the variance. Adding intraday temporal structure (Comparison; M1) explained 56.8% of variance ($\Delta R^2 = 0.568$). Incorporating seasonal phenological structure (Phenological period; M2) increased explained variance to 88.1% ($\Delta R^2 = 0.313$). Including flowering season and interactions (M3) resulted in only a minor increase to 90.1% ($\Delta R^2 = 0.020$). These results indicate that the majority of variation in interaction β-diversity is attributable to intraday temporal structure, while seasonal phenological and flowering season effects contribute much less. The full model's conditional $R^2 = 0.932$ confirms that random plot-to-plot variation adds relatively little additional explanatory power.

Model step	Biological meaning	Fixed effects added	R^2 marginal	ΔR^2	Cumulative R^2
M0	Spatial baseline (i.e., plot as random effect)	—	0.000	—	0.000
M1	Intraday temporal structure	Comparison among daily periods	0.568	**0.568**	0.568
M2	Seasonal phenological structure	* Phenological period (i.e., early-, mid-, late-season)	0.881	**0.313**	0.881
M3	Flowering season & interactions	* Flowering season (i.e., first and second season)	0.901	**0.020**	0.901

Conditional R^2 (full model) = 0.932; Marginal R^2 (full model) = 0.901.

References

Ballarin, C. S. Amorim, F. W. Arroyo-Correa, B. & Jordano, P. (2026). Floral resource diversity drives spatiotemporal variation in plant–pollinator network structure. *Oikos*, DOI: 10.1002/oik.11730.

Nakagawa, S., & Schielzeth, H. (2013). A general and simple method for obtaining R2 from generalized linear mixed-effects models. Methods in ecology and evolution, 4(2), 133-142.